Aus dem Medizinischen Zentrum für
Hals-, Nasen- und Ohrenheilkunde
Geschäftsführender Direktor: Prof. Dr. med. Jochen A. Werner
des Fachbereichs Medizin der Philipps-Universität Marburg
in Zusammenarbeit mit dem Universitätsklinikum Gießen und Marburg GmbH,
Standort Marburg

Nef from SIV_{mac239} down-modulates cell surface CXCR4 in tumor cells and inhibits proliferation, migration and angiogenesis

Inaugural-Dissertation
zur
Erlangung des Doktorgrades der gesamten Humanmedizin
dem Fachbereich Medizin der Philipps-Universität Marburg
vorgelegt von

Chengzhong Cai
aus Shanghai, China

Marburg, 2012

Angenommen vom Fachbereich Medizin der Philipps-Universität Marburg

am: 06.01.2012

Gedruckt mit Genehmigung des Fachbereichs

Dekan: Prof. Dr. med. M. Rothmund

Referent: Prof. Dr. med. R. Mandic

Korreferent: Prof. Dr. med. U. Wagner

Table of contents

1. Introduction

1.1 CXC Receptor 4

Chemokines, a family of small (8–14kDa) proteins secreted by cells, play a crucial role in the host immune defense system and are the major regulators involved in cell activation, differentiation and trafficking [26;50]. Depending on the spacing of their first two cysteine residues, chemokines are divided into four groups: C, CC, CXC and CX_3C chemokines. Chemokines bind and activate a subset of specific G-protein-coupled seven-span transmembrane receptors (chemokine receptor) on the surface of target cells. Up to now, nearly nineteen distinct chemokine receptors have been reported in mammals. Similarly as described for the ligands, their cognate receptors are divided into four groups (CC, CXC, CX_3C and XC chemokine receptors) according to the chemokines they bind. Although most chemokines bind to multiple receptors and some receptors bind to more than one chemokine, the C-X-C chemokine receptor type 4 (CXCR4) takes stromal cell-derived factor-1α (SDF-1α) as its unique ligand. Reportedly, SDF-1α could also bind to CXCR7/RDC1, however this mechanism was not well defined [64;96].

CXCR4, also known as fusin or CD184, is a small protein encoded by the human *CXCR4* gene. CXCR4 has a short, acidic extracellular N-terminal end, seven helical transmembrane domains with three intracellular hydrophilic loops [2]. As typically observed for G-protein linked receptors, the intracellular C-terminus of CXCR4 interacts with G-proteins and thereby enables transmembrane cell signaling after SDF-1α binding. CXCR4/SDF-1α activates numerous intracellular signaling pathways [28;63;91;97], such as the pI3K/AKT, cAMP/PKA, Ras/MAPK and DG/Ca^{2+}-PKC pathways, influencing cell chemotaxis, migration, proliferation, apoptosis and adhesion (Fig. 1).

CXCR4 is also known as a co-receptor for HIV/SIV during viral entry [17;18;73]. CXCR4/SDF-1α plays a central role in hematopoietic stem cell

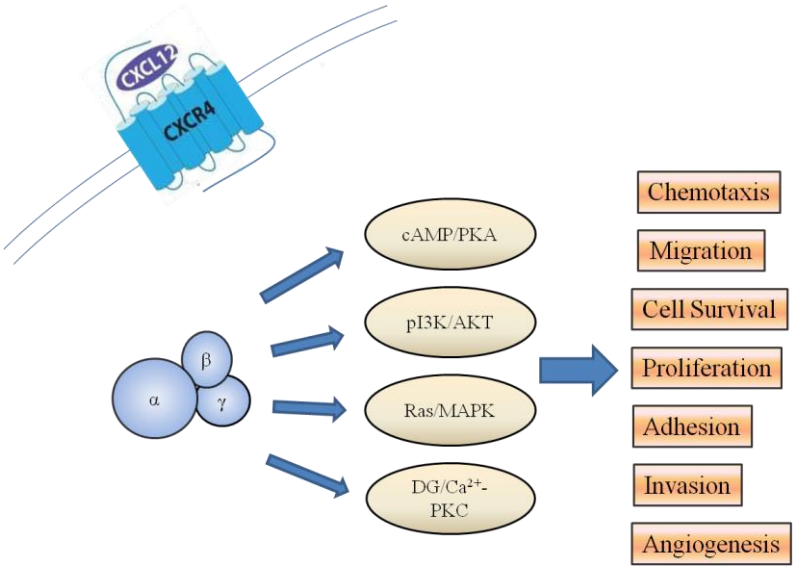

Figure 1. CXCR4/SDF-1α signal pathway. CXCR4/SDF-1α activates G-proteins and subsequently enables transmembrane cell signaling [29;65;96;101].

homing and bone marrow release. Knockout of CXCR4 or SDF-1α in transgenic mice results in embryonic lethality and underscores its critical role in the development of the nervous, cardiovascular as well as the hematopoietic system [57;79]. CXCR4 is found over expressed in a wide variety of human cancers, such as lung, pancreatic, breast, prostate and kidney cancer [4;5;30;48;62;88]. It is not surprising that more and more evidence indicates CXCR4/SDF-1α to play an important role in tumor development since it not only promotes cancer cell proliferation, migration but also metastasis and tumor angiogenesis [74;77].

Two CXCR4 variants (CXCR4 and CXCR4-Lo) have been identified so far. CXCR4-Lo, also known as variant 1, differs from the known human CXCR4 (variant 2) by the first 9 aa in the N-terminal extracellular domain of the receptor (Fig. 2), which is close to the region (aa 2-25) critical for SDF-1α binding [25;36;95]. The function of CXCR4-Lo is not well understood. However single reports see a lower tissue expression and reduced response to its ligand SDF-1α [36].

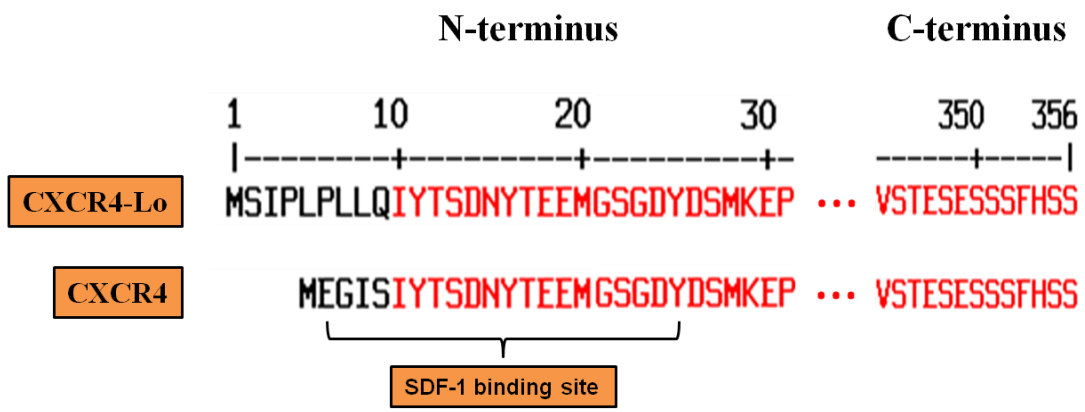

Figure 2. CXCR4 transcript variants. CXCR4-Lo differs from CXCR4 by the first 9 aa in its N-terminus which is close to the SDF-1 binding site.

*Figure is designed with the MultAlin software tool [21].

1.2 Negative regulatory factor (Nef)

Negative regulatory factor (Nef) is a 27kDa, N-terminal myristoylated protein. Nef is one of four accessory proteins expressed by primate lentiviruses, such as human immunodeficiency viruses -1 and -2 (HIV-1 and HIV-2) and simian immunodeficiency virus (SIV) (Fig. 3) [27].

Although Nef was originally called "negative factor," subsequent studies revealed that Nef was essential for high viral loads thereby promoting the development of acquired immunodeficiency syndrome (AIDS). Nef enhances viral infectivity during the early stage of the infection [1;92]. It is found highly expressed during the early phase of HIV infection and its mRNA is estimated to represent 75% of the early viral mRNA load [37;47]. HIV-1 harboring wild type Nef was found to be 5 to 20 times more infective than Nef-defective HIV-1 [19;45]. Nef can down-modulate cell surface MHC-I, MHC-II and CD28 to promote immune-escape of HIV infected cells since down modulation of these surface markers reduces viral antigen presentation at the cell surface

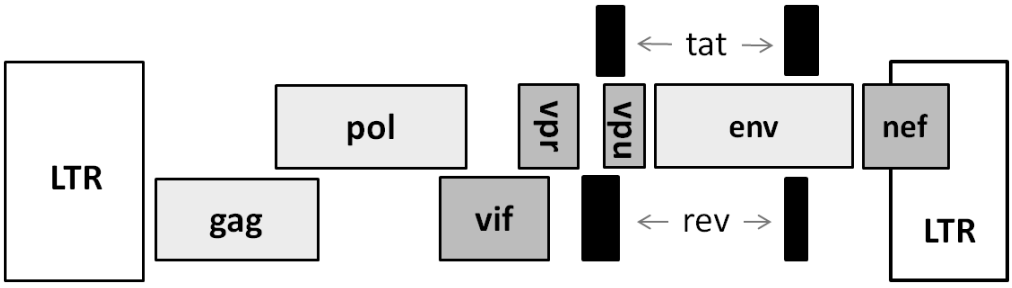

Figure 3. Proteins encoded by HIV/SIV. Except for the three prototypical retroviral proteins (Gag, Pol and Env) and two regulatory proteins (Tat, Rev), HIV/SIV also encodes four accessory proteins called Vif, Vpr, Vpu and Nef.

*Picture modified from Frankel et al. [27].

[9;33;51;76;82;83;86;87]. Correspondingly, lower surface levels of CD28 ensure that infected cells can not provide effective help following TCR engagement [7;89]. Moreover, Nef can not only promote apoptosis in T cells [80] but also is able to protect infected cells from apoptosis by inhibiting its internal [12;31;35] and external death signals [101]. Reportedly Nef can also inhibit p53 dependent apoptosis [34].

Nef is known to down modulate CD4, the main receptor for HIV/SIV as well as its co-receptor CCR5, aiming to prevent a lethal viral superinfection [65]. Nef was also reported as a wide-range regulator of chemokine receptors being able to reduce all surface levels of CC- and CXC- family members by up to 92% [66]. Nef down regulates CXCR4 from the surface of target cells and, as described for CD4 and CCR5, promotes resistance of the infected cells to superinfection [94;100]. Nef from different viral strains exhibits large differences in their ability to down regulate CXCR4. For example, Hrecka et al. [40] observed a strong down modulating effect of Nef from SIV_{mac239} and HIV-2 on cell surface CXCR4 and SDF-1α dependent lymphocyte metastasis. In

contrast, HIV-1 Nef did not exhibit a comparable effect. Similar effects could also be observed in CHO cells [94]. However, Venzke et al. did not observe such differences between HIV and SIV Nef [55].

Several studies addressed the mechanism underlying the Nef dependent down regulation of these receptors. The tyrosine- and dileucine- based motifs near the N-terminus and the C-terminal flexible loop in SIV- or HIV-2- Nef play a critical role for Nef dependent receptor internalization [8;10;55;78]. Mutations of critical residues in these regions could decrease cell surface internalization of CD4 and viral infectivity [58].

1.3 Aim of the study

Since Nef can down modulate surface CXCR4 in $CD4^+$ T cells, it is of interest to evaluate if Nef can also affect expression of this receptor in CXCR4 positive tumor cells and subsequently influence tumor-promoting features such as proliferation, migration and angiogenesis.

In this study, the CXCR4 positive tumor cells were transfected with Nef from SIV_{mac239} (SIV-Nef) and cell surface receptor levels were monitored by FACS analysis. Real time proliferation and migration of Nef transfected cells were measured with the xCELLigence system. Effects of Nef on angiogenesis were evaluated by an *in vitro* tube formation assay using HUVEC cells and its influence on cell signaling was evaluated in this study. Our data indicate that SIV-Nef could serve as an interesting experimental tool for the study of CXCR4-expressing tumors and potentially could help to pinpoint new therapeutic approaches for the treatment of CXCR4 positive tumors.

2. Materials

2.1 Chemicals and reagents

- Acetic acid glacial 100% (Merck,Darmstadt)
- Agar, Select (Sigma-Aldrich, St. Louis, MO, USA)
- Agarose (Invitrogen Life Technologies, Scotland, UK)
- Ammonium persulfate (APS) (Sigma-Aldrich, St. Louis, MO, USA)
- Ampicillin (Sigma-Aldrich, St. Louis, MO, USA)
- BSA (PAA Laboratories, Pasching, Austria)
- DAPI (Roche Diagnostics, Indianapolis, IN, USA)
- DMEM (PAA Laboratories, Pasching, Austria)
- DNA EcoRI Digest (DNA Marker) (New England Bio Labs, Beverly, MA, USA)
- DNA Hind III Digest (DNA Marker) (New England Bio Labs, Beverly, MA, USA)
- Dulbecco's Phosphate-Buffered Saline PBS (Biochrom AG, Berlin)
- Dodecylsulfate (Serva Electrophoresis, Heidelberg)
- EDTA (Roth, Karlsruhe)
- Ethanol (Roth, Karsruhe)
- Ethidiumbromide 1% (Roth, Karlsruhe)
- Fluorescent Mounting Medium (Dako Cytomation , Carpinteria, Foster City, CA, USA)
- Glycerol (Roth, Karlsruhe)
- Isopropanol (Acros Organics, Belgium, NJ, USA)
- Isopropyl-β-D-Thiogalacto-Pyranoside (IPTG) (Sigma-Aldrich, St. Louis, MO, USA)
- Skim milk powder (Merck, Darmstadt)
- 2-Mercapto-Ethanol (Sigma-Aldrich, St. Louis, MO, USA)
- Methanol (Sigma-Aldrich, St. Louis, MO, USA)
- Sodium-Chloride (Merck, Darmstadt)

- Sodiumhydroxide (Fisher Scientific, Leicestershire, UK)
- Nonidet P40 Substitute NP40 (Sigma-Aldrich, St. Louis, MO, USA)
- Penicillin-Streptomycin-Lincomycin (Invitrogen Life Technologies, Karlsruhe)
- Pierce ECL Western Blotting Substrate (Thermo Scientific, Rockford, IL, USA)
- Precision Plus Protein All Blue Standards (Bio-Rad Laboratories, München)
- Propidium Iodide (Sigma-Aldrich, St. Louis, MO, USA)
- Protein Assay Dye Reagent Concentrate (Bio-Rad Laboratories, München)
- Medical X-ray film (Agfa-Gevaert, Mortsel, Belgium)
- Ribonuclease A (Sigma-Aldrich, St. Louis, MO, USA)
- Rotiphorese Gel 30 (Roth, Karlsruhe)
- Hydrochlorid acid (Merck, Darmstadt)
- Tetramethylethylenediamine, TEMED (Roth, Karlsruhe)
- Tris-HCL (Roth, Kalsruhe)
- Trypsin-EDTA (PAA, Laboratories, Pasching, Austria)
- Tryptone EZMix (Sigma-Aldrich, St. Louis, MO, USA)
- Tween-20 (Roth, Karlsruhe)
- X-Gal (Sigma-Aldrich, St. Louis, MO, USA)
- Yeast Extract EZMix (Sigma-Aldrich, St. Louis, MO, USA)

2.2 Culture media

- Dulbecco's Modified Eagle Medium (DMEM) supplemented with:

  10% Fetal Calf Serum (FCS)

  1% L-glutamine

  100U/ml penicillin

  100mg/ml streptomycin

- EGM®-2 Endothelial Cell Growth Medium-2 (Lonza, Switzerland) supplemented with:

  Growth factors, cytokines, and other supplements (SingleQuots® Kit, CC-4176, Lonza)

- Lysogeny broth (LB) Medium (pH 7.0) for 1L:

NaCl	5.0g
Yeast	5.0g
Tryptone	10.0g
Agar-Agar (only for LB plate)	15.0g

2.3 Cell lines

- African Green Monkey SV40-transformed kidney fibroblast cell line (COS-7)
- CXCR4 expressing cell line designated HeLa-$_{ACC}$, see 3.2
- Human Umbilical Vein Endothelial Cells
  (HUVEC, C-003-5C, Life Technologies Corporation, Carlsbad, CA, USA)
- Madine-Darby canine kidney cell-clone 7 (MDCK-C7)
- Melanoma cell line (A7)
- HeLa cell line

2.4 Antibodies

2.4.1 Primary antibodies

- Anti-β-Actin (Sigma, St. Louis, MO,USA)
- Anti-Erk1/2 (Upstate, Lake Placid, NY, USA)
- Anti- Erk1/2-phospho (Sigma St. Louis, MO,USA)
- Anti-CXCR4 (Abcam plc, Cambridge, UK)
- Anti-Cyclin-D1 (Santa Cruz Biotechnology, Santa Cruz, CA, USA)

- Anti-SIV-Nef (Santa Cruz Biotechnology, Santa Cruz, CA, USA)
- Anti-Caspase 3 (Santa Cruz Biotechnology, Santa Cruz, CA, USA)
- Anti-Stat3 (Santa Cruz Biotechnology, Santa Cruz, CA, USA)
- Anti-Stat3-phospho (Santa Cruz Biotechnology, Santa Cruz, CA, USA)

2.4.2 Secondary antibodies

- Anti-mouse-IgG, HRP-linked antibody (Santa Cruz Biotechnology, Santa Cruz, CA, USA)
- Anti-rabbit-IgG, HRP-linked antibody (Santa Cruz Biotechnology, Santa Cruz, CA, USA)
- Anti-goat-IgG, HRP-linked antibody (Santa Cruz Biotechnology, Santa Cruz, CA, USA)

2.5 Kits

- First strand cDNA-Synthesis Kit (Roche Diagnostics, Mannheim)
- QIAgen RNeasy Mini Kit (Qiagen, Hilden)
- QIAquick Gel Extraction Kit (Qiagen, Hilden)
- QIAprep spin Miniprep Kit (Qiagen, Hilden)
- QIAprep plasmid Midiprep Kit (Qiagen, Hilden)
- Blood & Cell Culture DNA Mini Kit (13323, Qiagen, Hilden)
- REDTaq® ReadyMix™ PCR Reaction Mix (Sigma-Aldrich, St. Louis, MO, USA)
- StrataClone PCR Cloning Kit (Stratagene Products Division, La Jolla, CA, USA)
- Endothelial Tube Formation Assay (in Vitro Angiogenesis) kit (Cell Biolabs Inc., San Diego, CA, USA)
- *In vitro* angiogenesis kit (Cell Biolabs Inc., San Diego, CA, USA)

- CXCR4 specific siRNA (sc-35421) (Santa Cruz Biotechnology, Santa Cruz, CA, USA)
- Control scrambled RNA (1027281) (Santa Cruz Biotechnology, Santa Cruz, CA, USA)

2.6 Buffers:

2.6.1 PCR buffers:

- 5x TAE-buffer (Tris-Acetat-EDTA):

Trisbase	24.2g
Acetic acid glacial	5.7ml
EDTA	3.7g
H_2O	1.0L

- DNA- Loading buffer (6x buffer for agarose gel electrophoresis):

Glycerol	5.0ml
Bromophenol blue	40.0mg
Xylene cyanol	40.0mg
EDTA	3.7mg

- Agarose gel (1%):

Agarose	1.0g
1x TAE buffer	100.0ml
Ethidium bromide 1%	6.0µl

- DNA size standard:

100bp/1kb ladder	1.0µl
H_2O	9.0µl
6 x DNA loading buffer	2.0µl

2.6.2 Buffers for SDS-PAGE and Western blot analysis:

- Lysis-buffer (NP40):

Tris-HCl pH 7.5	20.0mM
NaCl	50.0mM
Glycerol	10%
Nonidet P40	1%

- 10 x Electrophoresis-buffer for SDS-PAGE:

Tris Base	60.4g
Glycin	76.0g
SDS	20.0g
H_2O	2.0L

- Transfer buffer (pH 8.3):

Tris	3.03g
Glycin	14.4g
H_2O	2.0L

- Blocking buffer:

Skim milk powder	3.0g
PBS	100.0ml

- SDS polyacrylamide gel solution (Table 1):

Table 1. SDS polyacrylamide gel solution

SDS Gel (X4)	Total Volume (ml)	Water (ml)	Polyacrylamide (ml)	1.5M Tris (ml)	0.5M Tris (ml)	10% SDS (ml)	10% APS (ml)	TEMED (µl)
6% (Stack)	20	10.8	4.0	0	5	0.2	0.2	20
10%	40	15.8	13.4	10	0	0.4	0.4	40
12%	40	12.8	16.4	10	0	0.4	0.4	40

2.6.3 Incubation solution for immunocytochemistry (ICC):

PBS	100.0ml
BSA	3.0g
NP40	300.0µl

2.7 Oligo Primers

Primers used in this study (Table 2) were designed using the Primer Premier 5.0 software and online blast (www.ncbi.nlm.gov/tools/primer-blast). Primers were obtained from Invitrogen (Life Technologies GmbH, Darmstadt).

2.8 Equipment

- Autoradiography cassette — Agfa, Köln
- BD FACS Calibur Flow Cytometer — Becton Dickinson, Heidelberg
- Cell culture hood — Heraeus, Hanau
- Centrifuge (Labofuge 400R) — Medifuge Heraeus, Hanau
- Centrifuge universal (30 F) — Hettich, Tuttllingen
- Epithelial volt-ohmmeter for TEER — WPI, Sarasota, FL, USA
- Eppendorf Bio Photometer — Eppendorf-Netheler-Hinz, Hamburg
- E-Plate for xCELLigence system — Roche, Mannheim
- Freezer (-30°C) — PORRKA, Hollola, Finland
- Freezer (-86°C) — Sanyo, Bad Neudorf
- Gel Doc 2000 — Bio-Rad Laboratories GmbH, München
- Hotblock for Tubes — HCL HBT 130, Kobe, Japan
- Ice machine — Ziegra, Isernhagen
- Incubator Shaker — New Brunswick Scientific, Edison, NJ, USA
- Laser Scanning Microscope — Olympus, Hamburg

• Liquid blocker	Daido, Sangyo, Japan
• Microscope (Olympus A×70)	Olympus, Hamburg
• Mini electrophoresis system	Bio-Rad, Hercules, CA, USA
• Mini protean II dual slab cell	Bio-Rad, Hercules, CA, USA
• Nitrocellulose membrane	Schleicher-Schuell Biosci., Dassel
• Pipetting aid	Hirschmann, Eberstadt
• Pipetman	Gilson, Middleton, WI, USA
• Refrigerator (+ 4°C)	PORRKA, Hollola, Finland
• Thermocycler	Biometra, Göttingen
• Thin-Certs (0.4µm)	Greiner Bio-One, Frickenhausen
• Thermal Printer DPU 414	Eppendorf, NY, USA
• Ultraviolet Transilluminator	UVP, Upland, CA, USA
• Vortex (Genie 2) mixer	Scientific Industries, Bohemia, NY, USA
• xCELLigence	Roche, Mannheim
• X-ray film	Agfa, Köln

2.9 Software

• RTCR software 1.2.1.1002	ACEA Biosciences, San Diego, CA, USA
• Quantity One 4.6.2	Bio-Rad, Hercules, CA, USA
• FlowJo 7.6.1	Tree Star, Ashland, OR, USA
• Multiple sequence alignment	MultAlin online [21], Tolouse, France
• Primer premier 5.0	Premier Biosoft international, Palo Alto, CA, USA
• PlasMapper online 2.0	University of Alberta, Edmonton, Canada [23]

3. Methods

3.1 Generation of recombinant plasmids

Full-length wild type SIV_{mac239}-Nef cDNA (GenBank: M33262.1) and its mutants (M8, $Y_{28}A$, $Y_{39}A$, $Y_{28}A/Y_{39}A$, $DE_{184}AA$, $LM_{194}AA$, $DD_{204}AA$ and $DE_{184}AA/LM_{194}AA/DD_{204}AA$) were amplified by Polymerase Chain Reaction (PCR) using the previously published SIV_{mac239}-Nef constructs as templates [58]. Two full-length CXCR4 splice variants, CXCR4-Lo (NCBI Reference Sequence: NM_001008540.1) and CXCR4 (NCBI Reference Sequence: NM_003467.2), were derived from total RNA of HUVEC cells which are known to exhibit high CXCR4 expression levels. Briefly: total RNA from HUVEC cells was isolated with the RNeasy Mini Kit (Qiagen, Hilden, Germany) and reverse transcription was performed with the Transcriptor First Strand cDNA Synthesis Kit (Roche Applied Science, Basel, Switzerland) using 1µg of total RNA according to the manufacturer's protocol. Primers for subcloning into pcDNA3.1(+) and pDsRed-monomer-N1 vectors (Invitrogen Corporation, Carlsbad, CA, USA) contained a HindIII restriction site at the 5' end and an EcoRI restriction site at the 3' end (Table 2). PCR was performed for 40 cycles of: 1) 95°C for 30s, 2) 56°C for 1min and 3) 72°C for 1min.

PCR products were separated according to their size in 1% agarose gel. After gel purification (QIAquick Gel Extraction Kit, Qiagen, Hilden), the amplicon was double-digested with HindIII and EcoRI (New England Biolabs GmbH, Frankfurt am Main). PCR products were ligated with pcDNA3.1(+) and pDsRed-N1 previously linearized with the same enzymes. DH5α competent cells (Invitrogen Corporation, Carlsbad, CA, USA) were subsequently transformed with the respective vectors. After growing on Lysogeny broth (LB) plates in the presence of 100µg/ml ampicillin (for pcDNA3.1) or 50µg/ml kanamycin (for pDsRed-N1) overnight at 37°C, clones were picked and cultured overnight at 37°C with agitation (250rpm) in LB media containing the

respective antibiotic. The plasmid DNA was purified using the QIAprep Spin Miniprep Kit (Qiagen) and the correct insert size was confirmed by HindIII/EcoRI double digest and sequence analysis (4base lab GmbH, Reutlingen) (Fig. 4).

Table 2. Primer sequence

Primer ID		Primer sequence
SIV_{mac239}-Nef (WT/ M8)		
pcDNA3.1(+)	Forward	5‘-AAACTTAAGCTTGCCACCATGGGTGGAGCTATTT-3‘
	Reverse	5‘-TCTGCAGAATTCTCAGCGAGTTTCCTTC-3‘
pDsRed-N1	Forward	5‘-GAGCTCAAGCTTGCCACCATGGGTGGAGCTATTT-3‘
	Reverse	5‘-TCTGCAGAATTCGGCGAGTTTCCTTCTTG-3‘
CXCR4 /CXCR4-Lo		
Primer forward	Forward	5‘-AAACTTAAGCTTGCCACCATGTCCATTCCT-3‘
	Lo-Forward	5‘-AAACTTAAGCTTAGCCACCGCATCT-3‘
Primer reverse	Rev. pcDNA3.1(+)	5‘-GGCTAGGAATTCCATCTGTGTTAG-3‘
	Rev. pDsRed-N1	5‘-TCTGCAGAATTCGGCTGGAGTGAAAACTTGA-3‘

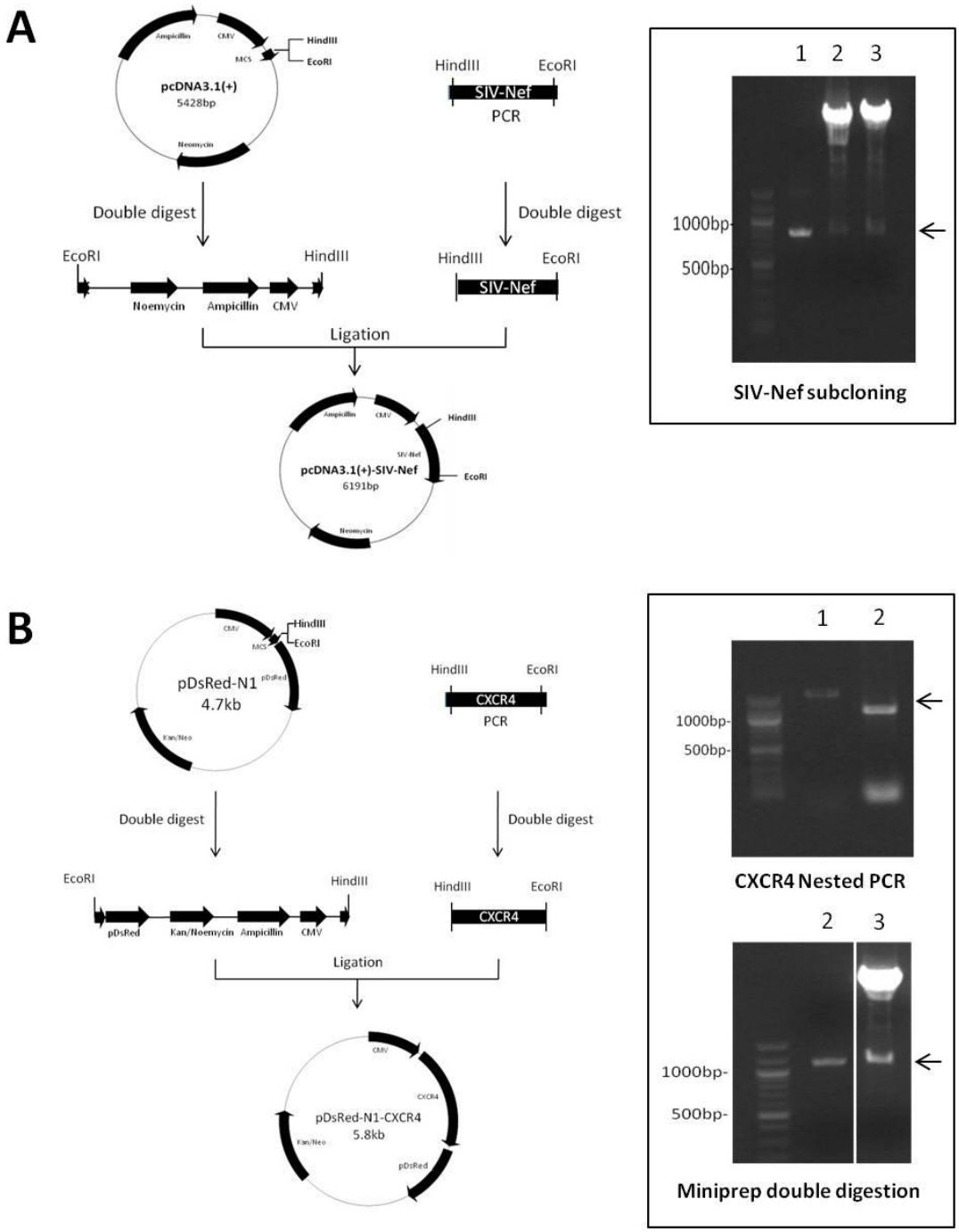

Figure 4. Generation of recombinant plasmids. (A) Subcloning of pcDNA3.1(+)-SIVmac239-Nef. 1) SIV-Nef PCR product; 2) HindIII/EcoRI double digestion of plasmid of Nef-WT; 3) HindIII/ EcoRI double digestion of plasmid of Nef-M8. **(B)** Cloning of pDsRed-N1-CXCR4. 1) PCR product amplified from HUVEC; 2) Nested PCR product amplified from 1:10 dilution of preceding PCR product; 3) HindIII/EcoRI double digestion of plasmid of pDsRed-N1-CXCR4. Arrow points to the respective Nef or CXCR4 DNA fragments.

*Picture is designed by PlasMapper 2.0 software tool [23].

Reaction system

- Reverse Transcriptase (RT) reaction system:

RNA	1.0µg
Oligo$(dT)_{18}$-Primer (50pmol/µl)	1.0µl
H_2O	up to 13.0µl
5x Reaction buffer	4.0µl
Desoxynucleotid-Mix (10mM)	2.0µl
RNAse Inhibitor (40U/µl)	0.5µl
Reverse Transkriptase (20U/µl)	1.0µl

- PCR reaction system:

Red Taq Mix	2.5µl
5`Primer (50nmol/µl)	0.5µl
3`Primer (50nmol/µl)	0.5µl
H_2O	10.5µl
Template	1.0µl

- Double digest reaction system:

PCR products (plasmid)	8.0µl
EcoRI (20U/µl)	0.5µl
HIND III (20U/µl)	0.5µl
10X NEB2 buffer	1.0µl

* 37°C water bath for 1 hour.

- Ligation system:

cDNA (gel purified)	6.5µl
10X T4 DNA ligase buffer	1.0µl
T4 DNA Ligase (400U/µl)	0.5µl
Linearized vector (gel purified)	2.0µl

* ligation overnight at 4°C.

3.2 STR analysis

The cell line ACC3 used in our study was obtained from Dr. Saku (Niigata University School of Dentistry, Japan) [15]. It reportedly was derived from an adenoid cystic carcinoma [39] and exhibits high CXCR4 expression levels [68]. Recently it was reported [75;105] that ACC3 cells were cross-contaminated with HeLa cells in different laboratories world-wide. In order to verify the cell line used in this study, DNA was isolated from ACC3 and HeLa cell lines using the Blood & Cell Culture DNA Mini Kit from Qiagen (13323, Hilden) and sent to a commercial provider for short tandem repeat (STR) analysis (DSMZ, Braunschweig). The data revealed that the ACC3 cell line was most closely related to HeLa cells as previously reported by Phuchareon et al. [75] (Table 3).

Therefore to distinguish the cells used in our studies from regular HeLa cells, although according to the STR analysis no significant difference should be expected, we designated the cells as HeLa-$_{ACC}$ during the course of our study. Since HeLa cells exhibit high cell surface expression levels of CXCR4 and were often used in research to evaluate the role of CXCR4 during the infection of HIV [11;93], HeLa-$_{ACC}$ cells should be suitable to evaluate the effect of SIV$_{mac239}$-Nef on tumor cell proliferation, migration and angiogenesis.

Table 3. STR analysis of the ACC3 cell line used in the study

Source	Cell Line	D5	D13	D7	D16	vWA	TH01	TPOX	CSF1	Amel	percent match to HeLa
DSMZ	HeLa	11,12	12, 13.3	8,12	9,10	16,18	7	8,12	9,10	X	100%
Phuchareon et al.*	HeLa	11,12	12, 13.3	8,12	9,10	16,18	7	8,12	9,10	X	100%
Phuchareon et al.*	ACC2/Sa	11,12	12, 13.3	8,12	9,10	16,17,18	7	8,12	9,10	X	97%
Phuchareon et al.*	ACC3	11,12	12, 13.3	8,12	9,10	17,18	7	8,12	9,10	X	94%
Our study	ACC3	11,12	12, 13.3	8,12	9,10	16,17,18	7	8,12	9,10	X	
Our study	HeLa	11,12	12, 13.3	8,12	9,10	16,18	7	8,12	9,10	X	

***** Data from: Phuchareon et al. [75]

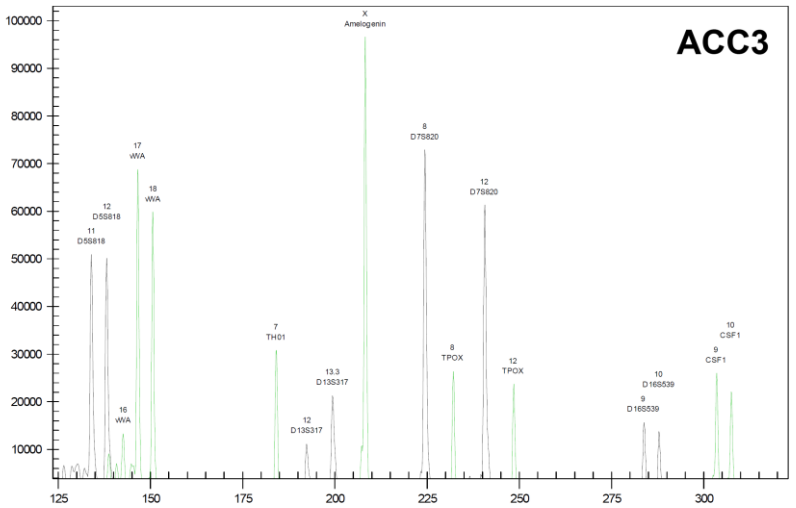

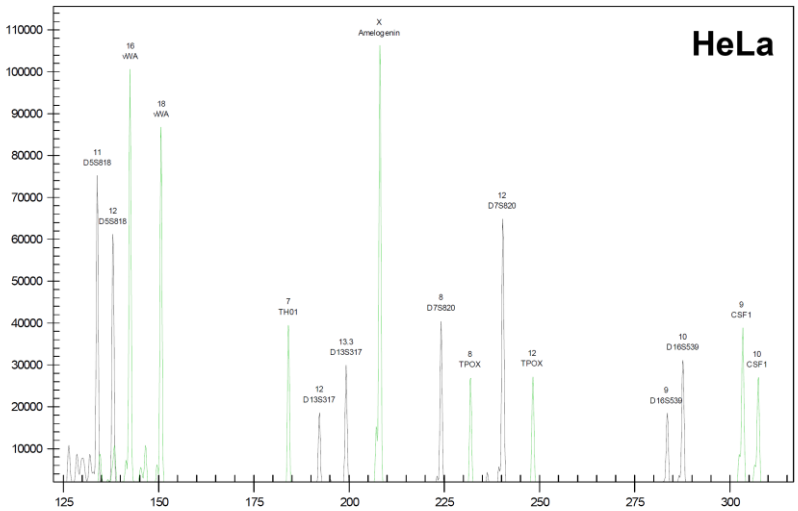

3.3 Cell culture and transfection

HeLa-$_{ACC}$, COS-7 [32] and MDCK-C7 [61;104] cells were cultured in Dulbecco's Modified Eagle Medium (DMEM) in the presence of 10% fetal calf serum (FCS), 1% L-glutamine, 100U/ml penicillin and 100mg/ml streptomycin at 37°C, 5% CO_2 in a humidified atmosphere. Human Umbilical Vein Endothelial Cells (HUVEC, C-003-5C, Life Technologies Corporation, Carlsbad, CA, USA) were cultured in EGM® -2 media supplemented with growth factors (Lonza Group Ltd, Basel, Switzerland). The culture medium was replaced every 3 days and the cells were passaged when reaching 80% confluence.

Twenty four hours before transfection, 5-10 x 10^5 cells were plated in 6 well cell culture plates. Cells were transfected after reaching 90-95% confluence. Cells were transfected with 4.0µg plasmid DNA using 10µl Lipofectamin™2000 (Invitrogen Life Technologies, Karlsruhe) per well according to the manufacturer's protocol (Table 4). The transfection medium was changed after 4-6 hours and cells were harvested 24 or 48 hours after transfection for further analysis. HUVEC cells were transfected using TransPass™ HUVEC Transfection Reagent (New England Bio Labs, Beverly, MA, USA) and Lipofectamin™ RNAiMAX (Invitrogen Life Technologies, Karlsruhe) was used for siRNA transfection according to the following protocols (Table 5 and Table 6):

Table 4. Transfection with Lipofectamin™ 2000

Culture vessel	Surf. Area per well (cm^2)	Shared reagents		DNA transfection	
		Vol. of plating medium (ml)	Vol. of dilution medium (ul)	DNA (µg)	Lipofectamin™ 2000 (µl)
12 well	4	1	2X100	1.6	4
6 well	10	2	2X250	4.0	10
60mm	20	5	2X500	8.0	20

Tab. 5 Transfection with TransPass™ V

Culture vessel	Vol. of plating medium (per well)	Conc. Of DNA in serum-free medium	HUVEC Reagent component in transfection complex mixture	TransPass V in transfection complex mixture
12 well	1ml	1.6µg in 150µl	1-2µl	1-4.0µl
6 well	2ml	3.0µg in 250µl	4-6µl	4-10µl
60 mm	5ml	6.0µg in 500µl	8-12µl	8-24µl

Tab. 6 Transfection with Lipofectamin™ RNAiMAX

Culture vessel	Surf. Area per well (cm^2)	Vol. of plating medium (ml)	Vol. of dilution medium (µl)	siRNA (pmol)	lipofectamin™ RNAiMAX (µl)
6 well	10	2.5	2 x 250	100	5
60mm	20	5	2 x 500	200	10

3.4 SDS-PAGE and Western blot

Forty-eight hours after transfection, cells were harvested, washed twice with PBS and then incubated in lysis buffer (1%NP-40, 20mM TrisCl pH 8.0, 137mM NaCl, 10% glycerol and 2mM EDTA) supplemented with protease and phosphatase inhibitor (Sigma-Aldrich. Saint Louis, MO, USA) [60]. After slow vortex at 4°C for 30min, lysates were centrifuged at 12,000x g at 4°C for 20min. The supernatant containing the total protein was transferred to a new tube and the protein concentration was determined with the Bradford method (Bio-Rad Laboratories, München).

Thirty-five µg total protein was separated by 10% sodium dodecyl sulfate polyacrylamide gel electrophoresis (SDS-PAGE) and then transferred to nitrocellulose membrane. The membranes were blocked in 3% milk/PBS for 1h at room temperature following an incubation with the primary antibodies at 4°C overnight. After washing with 3% milk/PBS thrice, membranes were incubated with an HRP-linked anti-rabbit or anti-mouse secondary antibody for 1h at room temperature. After washing away excessive antibody, bands were visualized with the enhanced chemiluminescence (ECL) method on x-ray film.

3.5 FACS analysis

Forty-eight hours after transfection, cells were harvested, washed twice in PBS/0.5% BSA and incubated with a PE-conjugated anti-CXCR4 antibody (PE Mouse Anti-Human CD184, BD Biosciences, San Jose, CA, USA) on ice for 1h. IgG2a was used as an isotype control. After wash, cell surface fluorescence was monitored by FACS analysis (BD LSR II, BD Biosciences, San Jose, CA, USA). 4'-6'-Diamino-2-phenylindole (DAPI) was added before checking and data analysis was performed using the FlowJo software (Tree Star, Inc., Ashland, OR, USA).

3.6 Confocal laser scanning microscopy

HeLa-$_{ACC}$ and COS-7 cells growing on cover slips were transfected with red fluorescent protein containing constructs (pDsRed-monomer-N1-CXCR4, pDsRed-monomer-N1-CXCR4-Lo, pDsRed-monomer-N1-Nef or pDsRed-monomer-N1-Nef-M8) and incubated for 48h. Cells were washed thrice in PBS, fixed for 30min in methanol (-20°C). The cover slips were sealed with clear nail polish and fluorescence was evaluated by confocal laser scanning microscopy (Fluoview, Olympus Deutschland GmbH, Hamburg).

HeLa-$_{ACC}$ cells that were grown on cover slips were transfected with Nef or control vector and incubated for 48h. Cells were washed thrice in PBS, fixed for 30min in methanol (-20°C) and incubated in staining buffer (3%BSA/0.3%NP40/PBS) for 30min. The respective anti-SIV-Nef or anti-CXCR4 antibodies were added (1:250) and incubated at room temperature for 2 more hours. Subsequently cells were washed thrice in staining buffer and secondary FITC-conjugated goat anti-rabbit IgG (for SIV-Nef) or TR-conjugated goat anti-mouse IgG (for CXCR4) were added (1:500) and incubated for 1h at room temperature in the dark. After washing thrice in staining buffer and once in water, DAPI (1:250) was added and incubated for 10min at room temperature. The cover slips were sealed with clear nail polish and subcellular localization was evaluated by confocal laser scanning microscopy.

3.7 In vitro scratch assay

HeLa-$_{ACC}$ cells transfected with SIV$_{mac239}$-Nef-WT or control (Nef-M8/ vector only) were seeded in 6-well plates and cell growth was allowed to continue until confluence was reached. The cell monolayer was scratched with a 100µl pipette tip and dislodged cells were washed away with PBS. Cell incubation was continued under standard conditions with medium containing

SDF-1α (100ng/ml) and the degree of cell migration into the scraped area was documented in the subsequent 72 hours [52].

3.8 Real time cell proliferation and migration

Tumor cell proliferation and migration was detected by the xCELLigence system (Roche, Mannheim, Germany). The presence of the cells on top of the electrodes will affect the local ionic environment at the electrode/solution interface, leading to an increase in the electrode impedance. The measured impedance, which is dependent on the level of confluence, was expressed as an arbitrary unit called the Cell Index (CI). The Cell Index at each time point is defined as (Rn-Rb)/(15Ω), where Rn is the cell-electrode impedance of the well when it contains cells and Rb is the background impedance of the well with the media alone. The increasing CI values were then recorded with the xCELLigence system in real-time to monitor cell proliferation and migration (Fig. 5.).

5 x 10^3 HeLa-$_{ACC}$ cells, transfected with the respective plasmid, were suspended in 150µl DMEM media and added into a 96-well plate that is specifically designed to measure cellular impedance (E-Plate, Roche, Mannheim). The attachment, spreading and proliferation of the cells were monitored every 15 minutes. SDF-1α (100ng/ml) was added to the media after 24 hours. Cells without SDF-1α were used as a negative control. Cell proliferation was monitored every 15 seconds for 6 hours and then every 15 minutes until maximum impedance was reached.

The cell monolayer was scratched when the impedance reached a maximum using a 10µl tip in the same way as described for the *in vitro* scratch assay above. The CI was monitored every 15 seconds for 6 hours then every 15 minutes for 24 hours. The CI at the time of the scratch was normalized and the proliferation curve was analyzed with the RTCA software (1.2.1.1002,

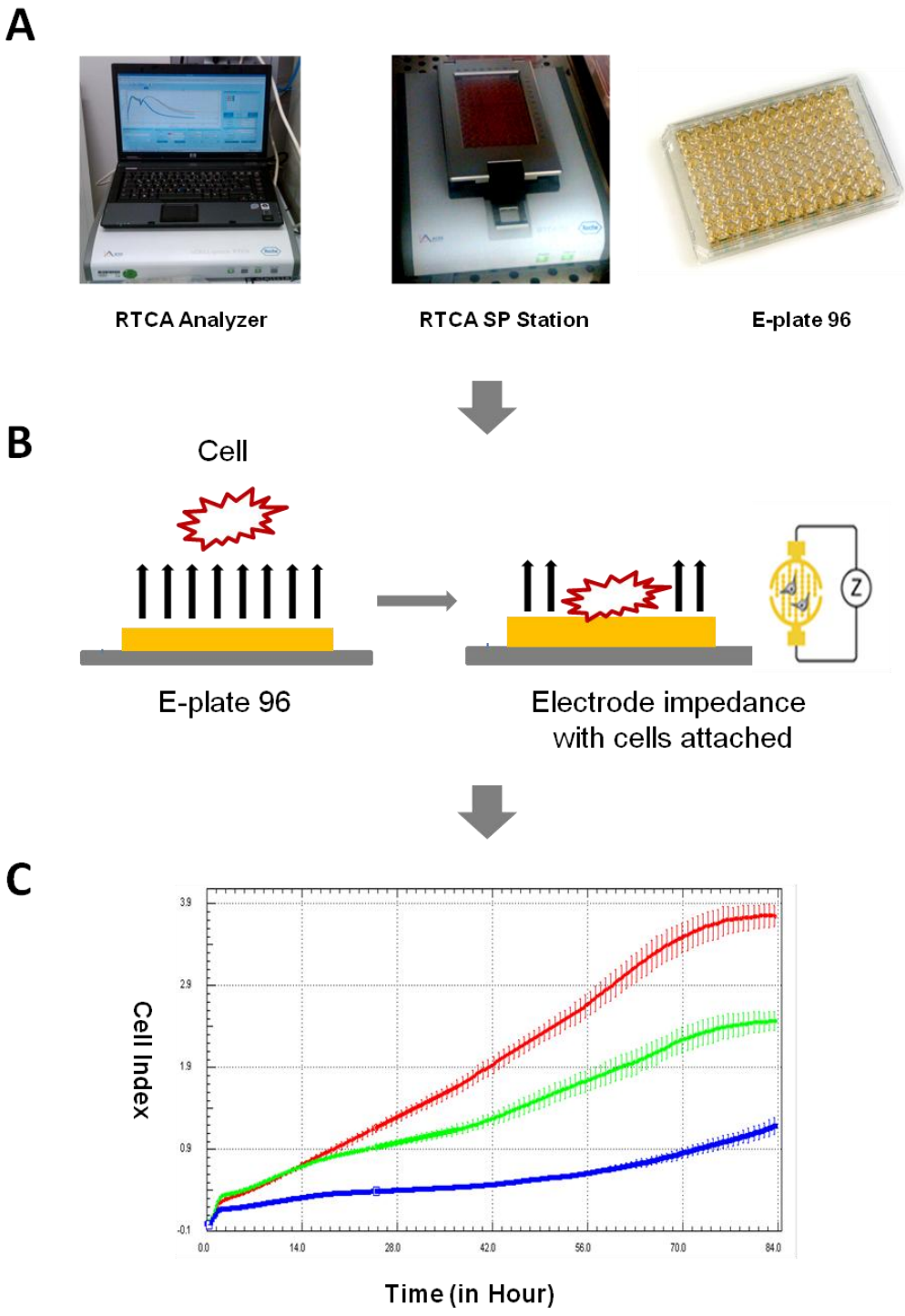

Figure 5. xCELLigence system. **(A)** The system consists of: real-time cell analysis (RTCA) Analyzer, RTCA SP Station, RTCA Control Unit and single use E-Plate 96. **(B)** Cells attaching on the top of the electrode increase the impedance. **(C)** Cell Index values, derived from the measured impedances, are continuously displayed with the Software.

(Modified from www.roch-applied-science.com/sis/xcelligence/index)

ACEA Biosciences, San Diego, CA, USA).

HeLa-$_{ACC}$ cells were transfected with SIV$_{mac239}$-Nef mutants (M8, $Y_{28}A$, $Y_{39}A$, $Y_{28}A/Y_{39}A$, $DE_{184}AA$, $LM_{194}AA$, $DD_{204}AA$ and $DE_{184}AA/LM_{194}AA/DD_{204}AA$) and their effects on cell proliferation were detected as described above.

3.9 Electrical resistance breakdown assay

The electrical resistance breakdown assay was used to measure cellular invasiveness. Madine-Darby canine kidney cells (MDCK) as described previously were used as a cellular barrier in TEER since they are able to form high transepithelial electrical resistance after reaching confluence [61;104].

The membrane filter cups having a pore size of 0.4µm and a culture surface of 4.25cm^2 (ThinCerts^{TM}, Greiner Bio-One, Frickenhausen) were inserted into a 6-well cell culture plate containing 3ml medium per well. 1 x 10^5 MDCK cells were then seeded into the filter cup to grow to confluence over 48 hours. The current-induced voltage change across the epithelial monolayer is displayed as resistance on a voltohmmeter (EVOM^{TM}, World Precision Instruments, Sarasota, FL, USA).

5 x 10^5 HeLa-$_{ACC}$ cells, 24h after transfection with Nef-WT, were seeded carefully on top of the MDCK monolayer. The same MDCK cells and Nef-M8 or vector-only transfected HeLa-$_{ACC}$ cells were seeded as a negative control, whereas highly invasive A7 Melanoma cells were used as a positive control [46;59;98]. All cells were grown in DMEM medium and SDF-1α (100ng/ml) was added to the medium of the lower chamber when cells were seed into the filter cups. TEER breakdown will occur, if the integrity of the MDCK monolayer is compromised by tumor cells [46].

3.10 Matrix gel invasion assay

Cell invasion was also measured by a matrix gel invasion assay. 24-well culture inserts (ThinCert^{TM}, Greiner Bio-One, Frickenhausen) with 8µm pores were inserted in a 24-well plate. ECM gel was thawed overnight at 4°C. 60µl ECM gel solution was added to each cell culture insert and dried at room temperature for 1h under laminar air flow. Nef-WT and CXCR4 siRNA transfected HeLa-$_{ACC}$ cells, as well as control HeLa-$_{ACC}$ cells were cultured in serum free DMEM (contained 0.2% BSA) one night before the invasion assay. Cells were harvested, washed twice in PBS and resuspended in serum-free medium (containing 0.2% BSA) at a final concentration of 1 X 10^6 /ml. 200µl of the cell suspension was added into the upper chamber and 600µl of DMEM with 10% FBS and 100ng/ml SDF-1α were added into the lower chamber. Cells were cultured for 20h at 37°C and 5% CO_2. Subsequently, the upper chamber was carefully taken out and the membrane was fixed in cold (-20°C) methanol for 30min. Then the membrane was stained with 0.5% Toluidine Blue for 20min at room temperature. Cells at the inner surface of the upper chamber were carefully wiped with a cotton swab. Invading cells were detected by light microscopy in the center of the bottom of the membrane and the average number of at least 3 fields per membrane was calculated.

3.11 Endothelial in vitro tube formation assay

In vitro angiogenesis assay was used to evaluate the effects of SIV-Nef on HUVEC cell tube formation. HUVEC cells were transfected with SIV-Nef-WT, CXCR4 or CXCR4 siRNA. pcDNA3.1(+), Nef-M8 or scrambled siRNA transfected HUVEC cells were used as a control. Twenty-four hours after transfection, 1 X 10^6 HUVEC cells were seeded into the ECM precoated 96-well plates and incubated at 37°C, 5% CO_2. Tube formation was observed

and evaluated by light microscopy 4-18 hours after seeding of the cells.

3.12 Statistical analysis

Nonparametric tests were used for data analysis. The Mann-Whitney test was implemented to evaluate the statistical significance of the proliferation rates between SIV-Nef-WT, Nef-M8 and vector-only transfected HeLa-$_{ACC}$ cells. A probability less than 0.05 ($p<0.05$) was considered statistically significant.

4. Results

4.1 Co-expression of SIV_{mac239}-Nef and CXCR4

Full length cDNAs of SIV_{mac239}-Nef-WT, SIV_{mac239}-Nef-M8 and CXCR4 were subcloned into the mammalian expression vector pcDNA3.1(+) and pDsRed-monomer-N1 as described in the Methods section (Fig. 4). To confirm expression of the constructs, COS-7 cells were transfected with the respective plasmids and protein expression was evaluated by Western blot analysis (Fig. 6).

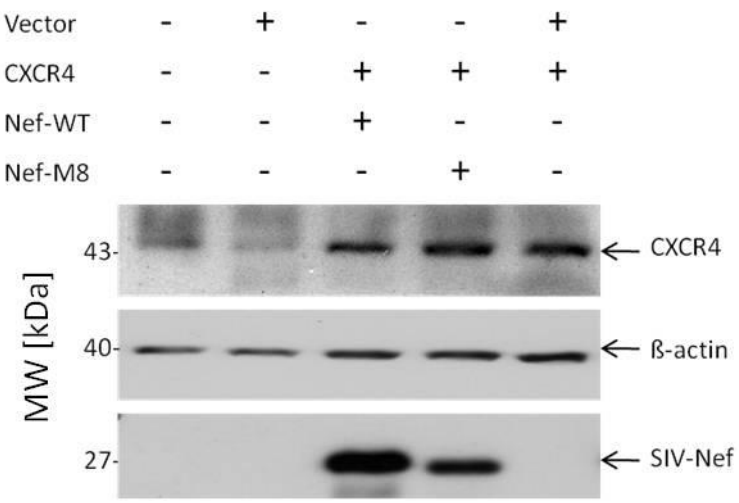

Figure 6. Exogenous expression of Nef and CXCR4 in COS-7 cells. Western blot analysis demonstrates co-expression of CXCR4 and Nef-WT or Nef-M8 in COS-7 cells after co-transfection of the respective two constructs. Cells transfected with CXCR4 and empty vector (control) express CXCR4 but exhibit no Nef signal, whereas untransfected cells do not express Nef or significant levels of endogenous CXCR4. No obvious change is noted in the total CXCR4 protein level after transfection with Nef. Actin was used as an internal control.

Nef (27kDa) and CXCR4 protein (43kDa) can be detected in Nef and CXCR4 transfected cells. No Nef was detectable in SIV-Nef untransfected cells. Only minimal amounts of endogenous CXCR4 were seen in untreated and pcDNA3.1(+) (“vector-only”) transfected control cells. No obvious change in whole cellular CXCR4 protein levels was seen after co-transfection with Nef.

Fluorescence microscopy demonstrates Nef-WT protein at the cell surface as well as in the cytoplasm of COS-7 cells, whereas the functionally defective Nef protein (Nef-M8) was found accumulated at the plasma membrane. CXCR4, as well as CXCR4-Lo, localize to the cell membrane, cytoplasm and even the nucleus (Fig. 7).

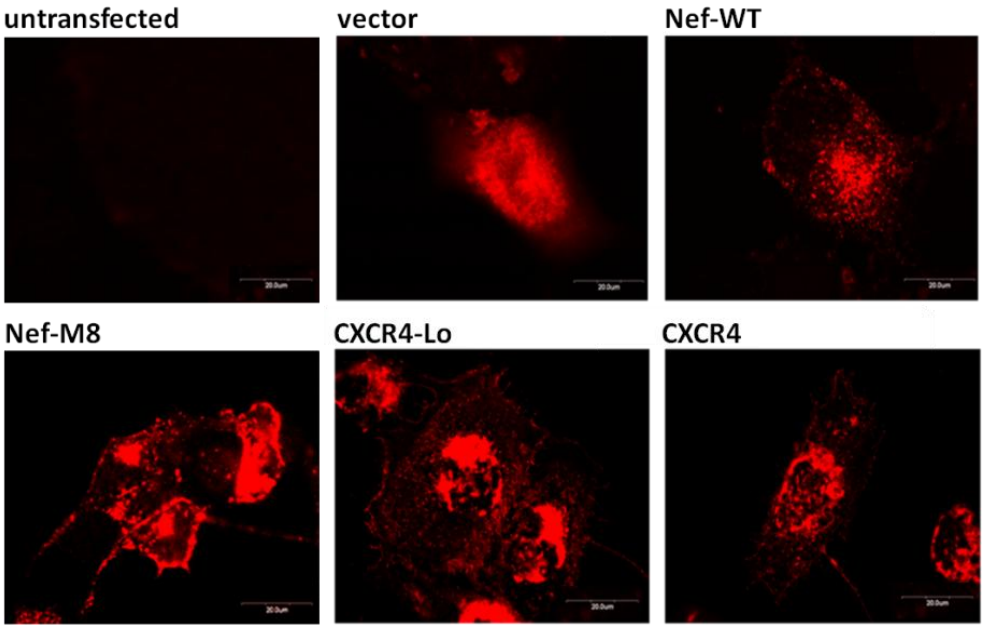

Figure 7. Fluorescence detection of COS-7 cells transfected with pDsRed-N1-Nef or pDsRed-N1-CXCR4 plasmids.

The surface expression level of CXCR4 in COS-7 cells was detected by FACS analysis. Compared with untreated COS-7 cells which had little or even no expression of surface CXCR4 (<2%), the expression level of surface CXCR4 was increased to app. 20% in CXCR4 or CXCR4-Lo transfected COS-7 cells (Fig. 8).

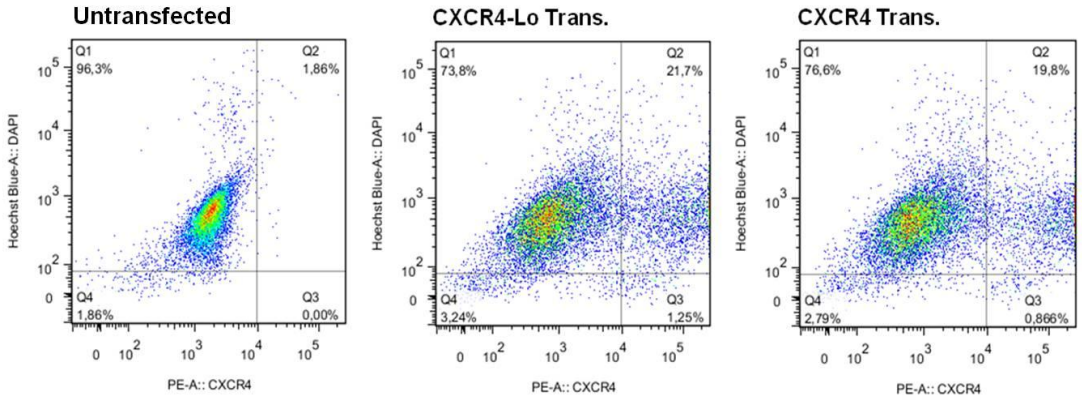

Figure 8. Expression of surface CXCR4/CXCR4-Lo in transfected COS-7 cells was evaluated by FACS analysis.

4.2 Co-transfection of CXCR4 and SIV_{mac239}-Nef leads to down regulation of CXCR4 from the cell surface in COS-7 cells

After demonstrating the expression of CXCR4 constructs in COS-7 cells, the same constructs were co-transfected with WT-Nef. Functionally deficient Nef-M8 and pcDNA3.1(+) (vector-only) were co-transfected with CXCR4 as a negative control. Although no change in whole cellular CXCR4 protein levels was detected (Fig. 6), FACS analysis revealed that cell surface fluorescence of CXCR4 was reduced in Nef-WT co-transfected cells, but not in Nef-M8 and vector-only co-transfected cells indicating a specific effect of Nef for down-modulation of the CXCR4 receptor from the cell surface. The reduction of CXCR4-Lo by Nef-WT was also detectable but not as pronounced as in CXCR4 transfected COS-7 cells (Fig. 9).

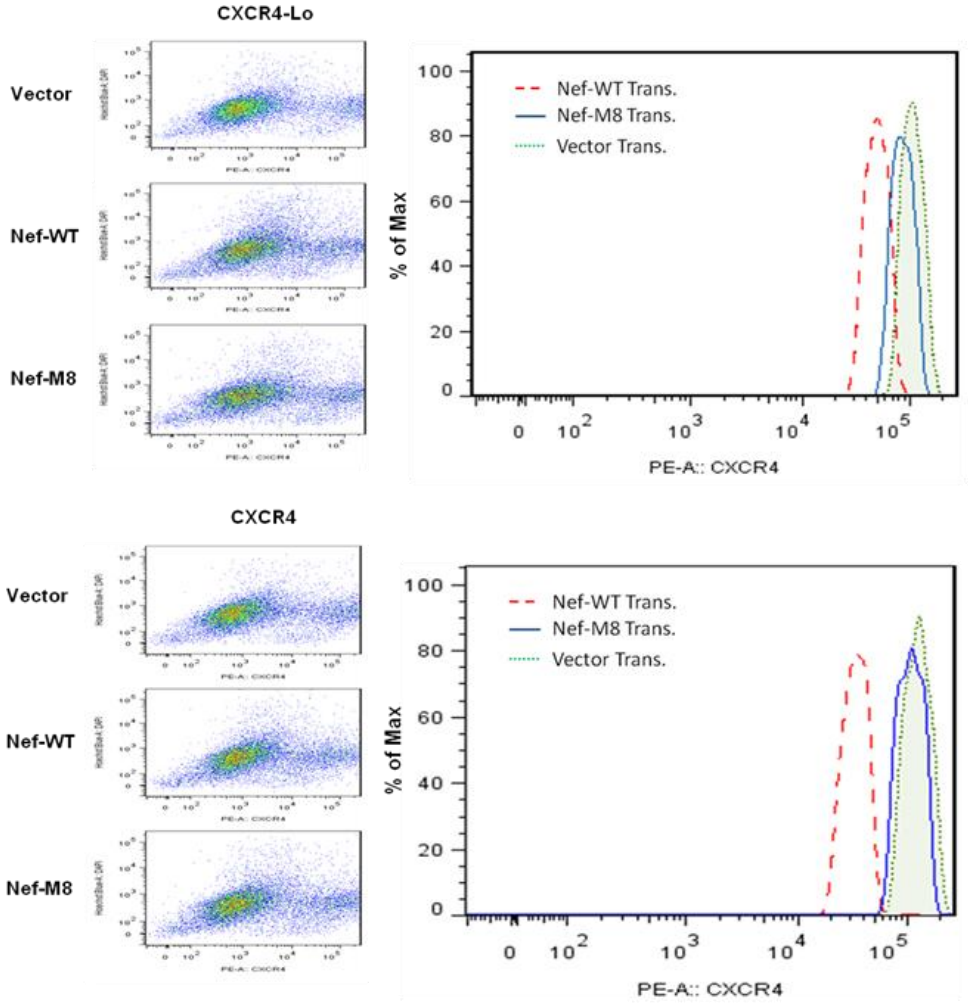

Figure 9. FACS analysis of COS-7 cells co-transfected with CXCR4 and Nef. COS-7 co-transfected with the two CXCR4 variants (CXCR4-Lo, CXCR4) and Nef-WT. Nef-M8 or pcDNA3.1(+) was used as a control. Surface CXCR4 expression was detectable after transfection. Both CXCR4 splice variants can be downregulated by Nef-WT, but not by Nef-M8 or vector control. The reduction of CXCR4-Lo by Nef-WT appeared less pronounced than in CXCR4 transfected cells.

4.3 SIV_{mac239}-Nef down-regulates endogenous CXCR4 from the cell surface of CXCR4 expressing tumor cells

In order to evaluate the effects of SIV-Nef on endogenous cell surface CXCR4, the CXCR4 positive tumor cell line, HeLa-$_{ACC}$, was transfected with SIV_{mac239}-Nef-WT or negative control (Nef-M8 or vector-only). Western blot analysis could detect Nef protein only in SIV-Nef transfected cells and could confirm high endogenous CXCR4 expression (Fig. 10). No procaspase-3 cleavage was detectable in Nef transfected HeLa-$_{ACC}$ cells. Similarly as observed in CXCR4 transfected COS-7 cells, there was no obvious change in total CXCR4 protein expression levels in SIV-Nef transfected HeLa-$_{ACC}$ cells.

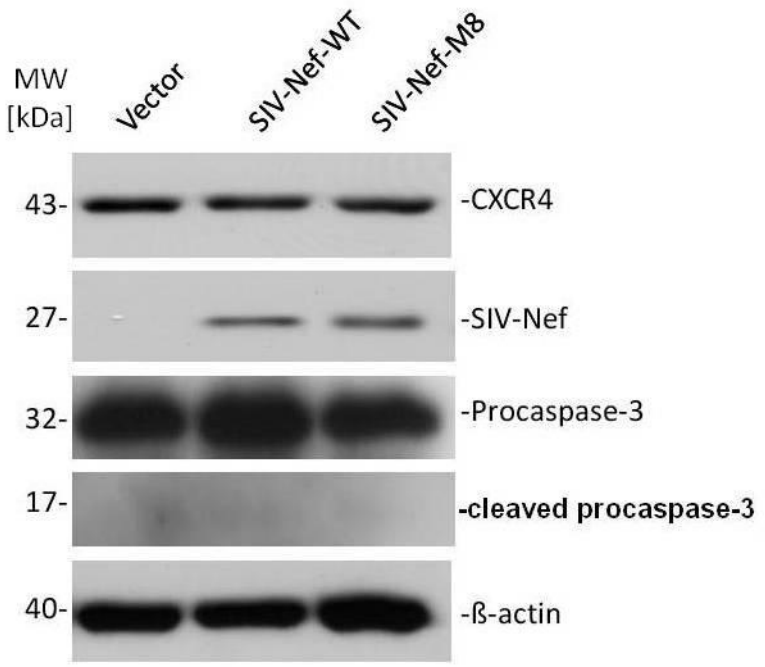

Figure 10. Western blot analysis of Nef-WT, Nef-M8 and vector-only transfecetd HeLa-$_{ACC}$ cells. All cells -transfected and untransfected- are positive for endogenous CXCR4, whereas only the Nef-transfected cells express the viral protein. No cleaved procaspase-3 is seen in Nef-transfected cells. Beta-actin was used as an internal control.

Immunocytochemical analysis demonstrated Nef in the cytoplasm and at the plasma membrane. Endogenous CXCR4 was detectable in all HeLa-$_{ACC}$ cells. Interestingly, similarly as observed in CXCR4 transfected COS-7 cells, a CXCR4-specific signal was not only found at the plasma membrane but also in the cytoplasm and nucleus (Fig. 11). No obvious co-localization of Nef and CXCR4 was detected (Fig. 11).

Similarly as observed for COS-7 cells, FACS analysis revealed a reduction of cell surface CXCR4 in Nef-transfected HeLa-$_{ACC}$ cells (Fig. 12).

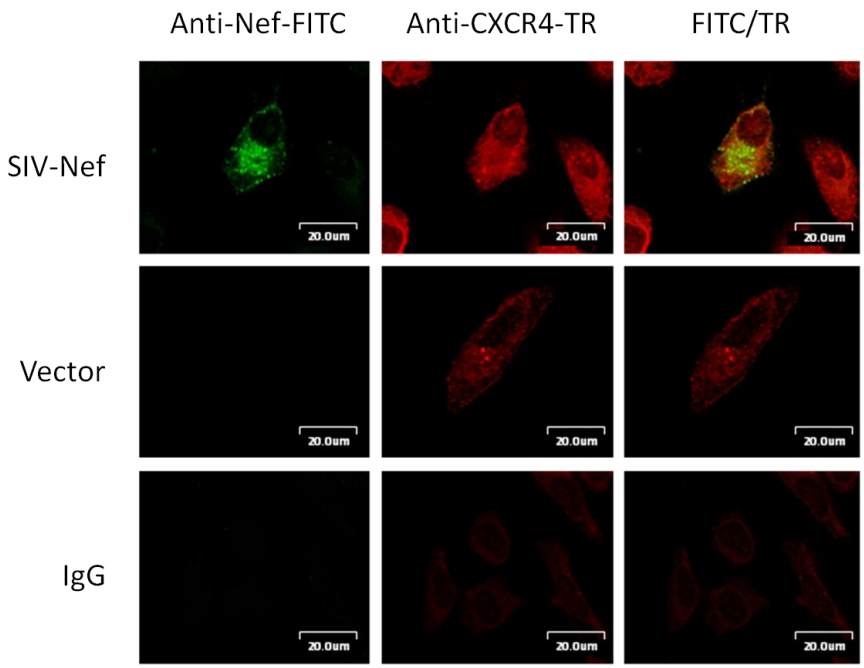

Figure 11. Immunocytochemical analysis of HeLa-$_{ACC}$ cells transfected with SIV-Nef. Using laser scanning microscopy, endogenous CXCR4 (TR) is found at the plasma membrane as well as in the cytoplasm and nucleus. SIV-Nef (FITC) is found at the plasma membrane and in the cytoplasm. No obvious co-localization of Nef and CXCR4 was detected

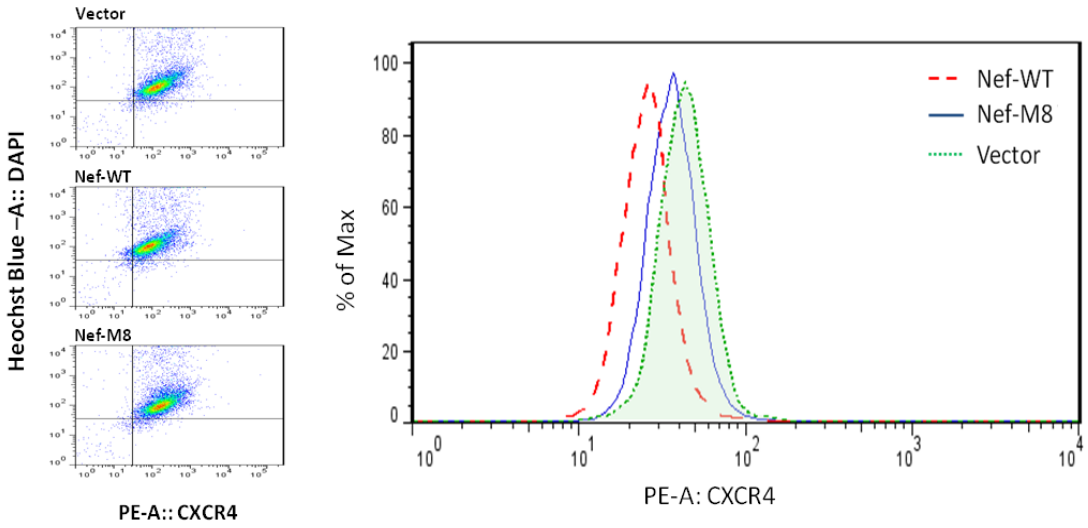

Figure12. FACS analysis of HeLa-$_{ACC}$ cells transfected with SIV-Nef. HeLa-$_{ACC}$ cells were transfected with Nef-WT and Nef-M8, pcDNA3.1(+). The latter two served as a negative control.

4.4 Proliferation of HeLa-$_{ACC}$ cells is reduced after Nef transfection

The xCELLigence system was deployed to measure real-time cell proliferation and migration. HeLa-$_{ACC}$ cells were transiently transfected with SIV-Nef-WT. Nef-M8, vector-only, CXCR4 siRNA and scrambled short RNA were used as a control. Transfected HeLa-$_{ACC}$ cells were seeded into specialized 96-well culture plates (E-plate) and electrode impedance was measured continuously as described in the Methods section (Fig. 5). Twenty-four hours after cell seeding, SDF-1α (100ng/ml) was added to the medium. Vector-only transfected control cells treated with SDF-1α exhibited an enhanced proliferation rate compared to SDF-1α untreated cells (Fig. 13).

The proliferation rate of the vector control was taken as a baseline (1.0) and the proliferation ratio of Nef-WT and Nef-M8 compared to the vector control (relative proliferation rate) was plotted to highlight potential effects of Nef (Fig. 14A). Nef-WT transfected HeLa-$_{ACC}$ cells exhibited a markedly reduced proliferation rate in both untreated and SDF-1α treated groups,

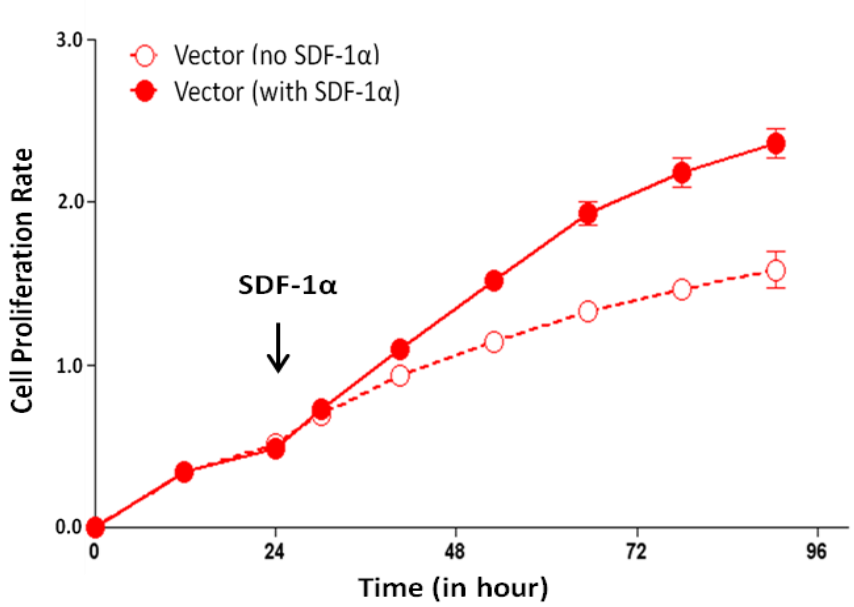

Figure 13. HeLa-$_{ACC}$ cells (vector control) exhibit an enhanced proliferation rate after addition of 100ng/ml SDF-1α.

whereas Nef-M8 transfected cells exhibited a similar proliferation rate as the vector-only transfected cells, pointing to a specific effect of the viral protein on HeLa-$_{ACC}$ cell proliferation. CXCR4 siRNA transfection resulted in inhibition of the cells proliferation rate compared to scrambled control RNA transfected cells (as baseline) (Fig. 14A).

Cell proliferation was monitored from 0 to 48 hours after cell seeding (Fig. 14B). The cell doubling time of Nef-WT transfecetd HeLa-$_{ACC}$ cells significantly increased from 30 hours to 45 hours (p=0.02) and this effect appeared even more pronounced in the SDF-1α treated cells (p=0.01), indicating that SIV-Nef significantly inhibits cell proliferation. Nef-M8 and vector-only transfected HeLa-$_{ACC}$ cells exhibited a decrease in doubling time after incubation with SDF-1α, whereas Nef-WT transfected cells did not respond significantly to SDF-1α, which appears to be in accordance with the observed decrease of surface CXCR4 by SIV-Nef.

cDNA from SIV_{mac239}-Nef M8, containing functionally relevant mutations at the N-terminus as well as C-terminal flexible loop [58] (Fig. 15A), was subcloned into pcDNA3.1(+) as described above. The construct was confirmed by sequence (Fig. 15A) and Western blot analyses (Fig. 15C). The effect of functionally deficient Nef on HeLa-$_{ACC}$ cell proliferation was evaluated by the xCELLigence system. The slope of the cell index curve was calculated and shown in the bar chart (Fig. 15B). Nef-M8 transfected cells have a similar proliferation rate as vector-only transfected cells and were used as a Nef negative control (set to 100%) to evaluate the effect of Nef-WT and the other mutants on cell proliferation (Fig. 15B). Wild type Nef on the other hand served as a positive control. As expected, Nef-WT decreased proliferation of transfected HeLa-$_{ACC}$ cells to 41% of negative control values (M8). The $Y_{39}AA$ mutant Nef showed a similar efficiency as Nef-WT (49%), whereas the $Y_{28}A$ (81%), $DE_{184}AA$ (62%), $LM_{194}AA$ (73%) and the triple mutation protein DELMDD ($DE_{184}AA/LM_{194}AA/DD_{204}AA$) (83%) Nef mutant lost most of their ability to inhibit cell proliferation. Interestingly, the $DD_{204}AA$ (102%) mutant exhibited an inhibition of cell proliferation comparable to Nef-M8.

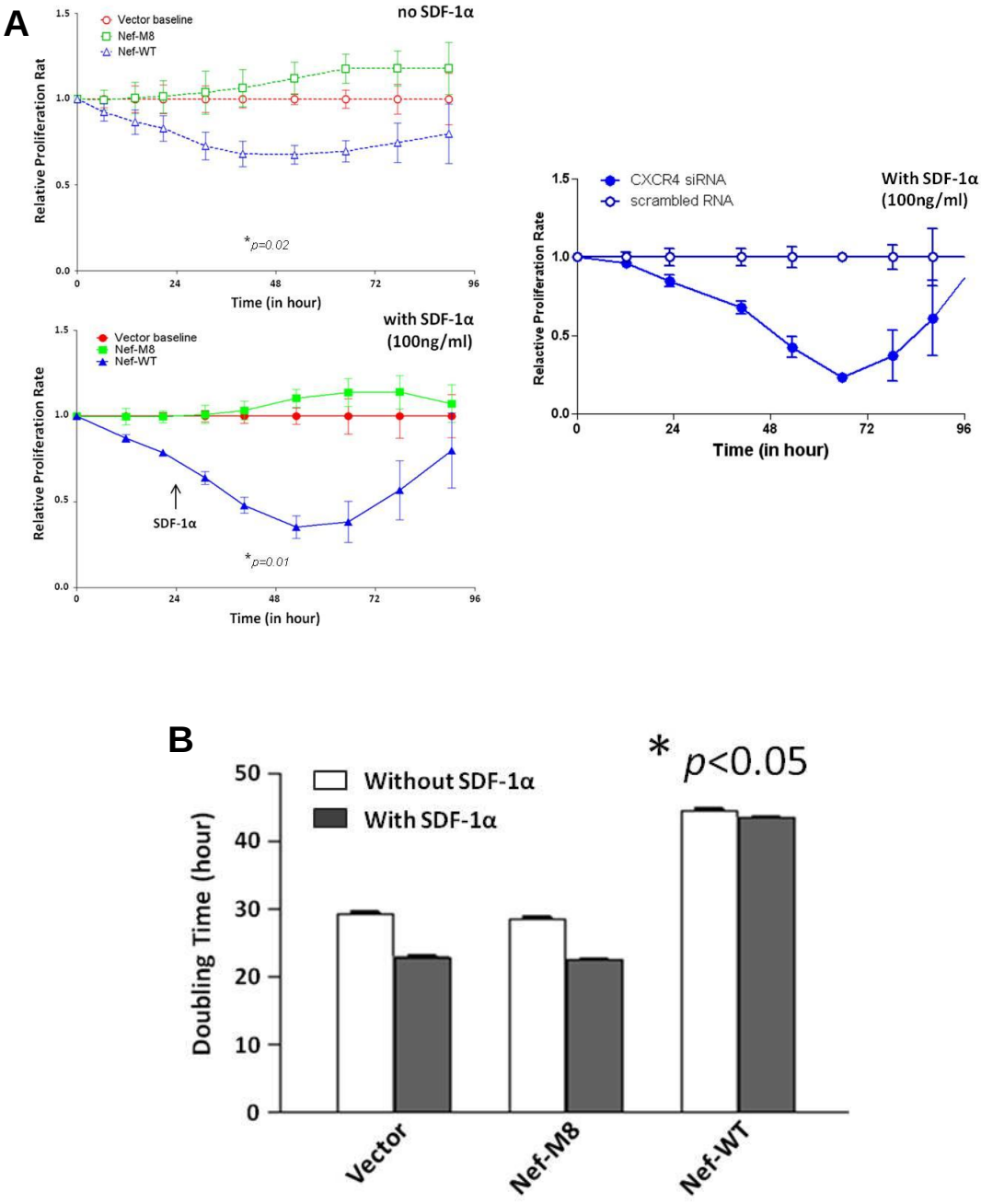

Figure 14. Nef from SIV_{mac239} inhibits proliferation of HeLa-$_{ACC}$ cells. A) The relative proliferation rate of Nef-WT and Nef-M8 transfected HeLa-$_{ACC}$ cells relative to the vector only transfected control cells, that were normalized to 1.0, reveals a significant (p=0.02 at 48h) inhibition of proliferation in the Nef-WT transfected cells. This effect appeared even more pronounced in the SDF-1α treated cells (p=0.01 at 48h). CXCR4 siRNA transfected HeLa-$_{ACC}$ cells also exhibited an obvious inhibition of proliferation rate compared to scrambled RNA (as baseline). **B)** Doubling time of transfected HeLa-$_{ACC}$ cells with and without SDF-1α treatment.

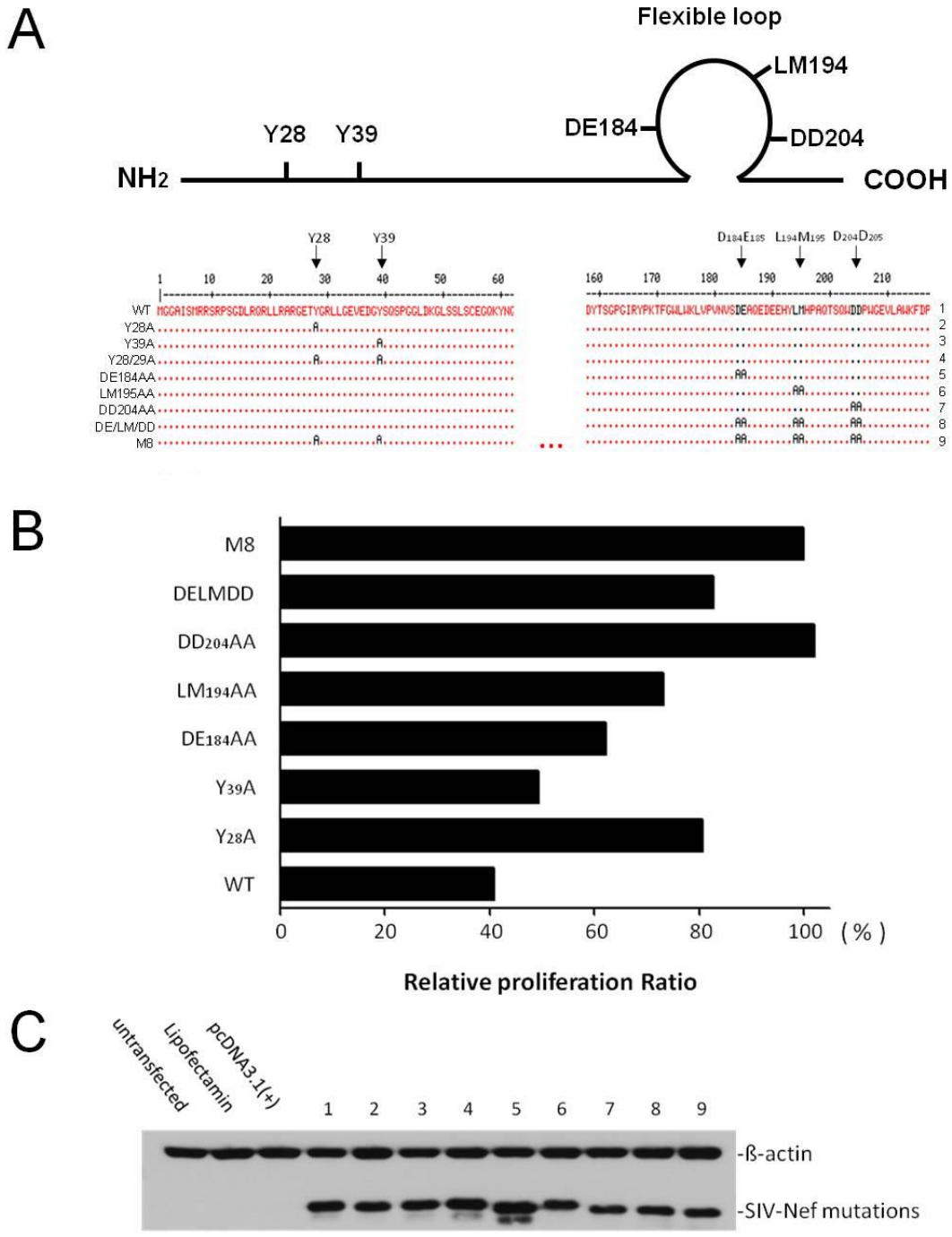

Figure 15. Effects of SIV_{mac239}-Nef mutations on cell proliferation. A) Location of Nef mutations in different endocytic motifs (modified from Mandic et al. Mol Biol Cell, 2001). Constructs were confirmed by sequence analysis. **B)** Effect of mutations in SIV_{mac239}-Nef on cell proliferation. Nef-M8 transfected HeLa-$_{ACC}$ cells were used as a negative control (set to 100%) and the ratio for the Nef mutants was calculated relative to this value. Nef-WT served as a positive control. **C)** Expression of transfected SIV-Nef was confirmed by Western blot analysis. ß-actin was used as an internal control.

4.5 Migration is inhibited in SIV_{mac239}-Nef transfected $CXCR4^+$ tumor cells

An *in vitro* scratch assay was performed to evaluate the potential influence of Nef on cellular migration. Cell numbers were normalized for better comparison. After scratching the cell layer with a pipette tip, the subsequent rise in impedance was the lowest in the Nef-transfected HeLa-$_{ACC}$ cells compared with vector-only or Nef-M8 transfected cells pointing to Nef as an inhibitor of cell migration in HeLa-$_{ACC}$ (Fig. 16A). Considering the doubling time to be around 30-50 hours, the short time required for impedance to rise after scratching the cell layer indicates that migration rather than proliferation is likely responsible for this effect. Microscopical analysis of HeLa-$_{ACC}$ cells show a different rate of cells moving into the cell free scratched region. Nef-WT transfected cells displayed the lowest migratory ability compared with Nef-M8 or vector control pointing to an inhibitory effect of Nef on cell migration (Fig. 16B).

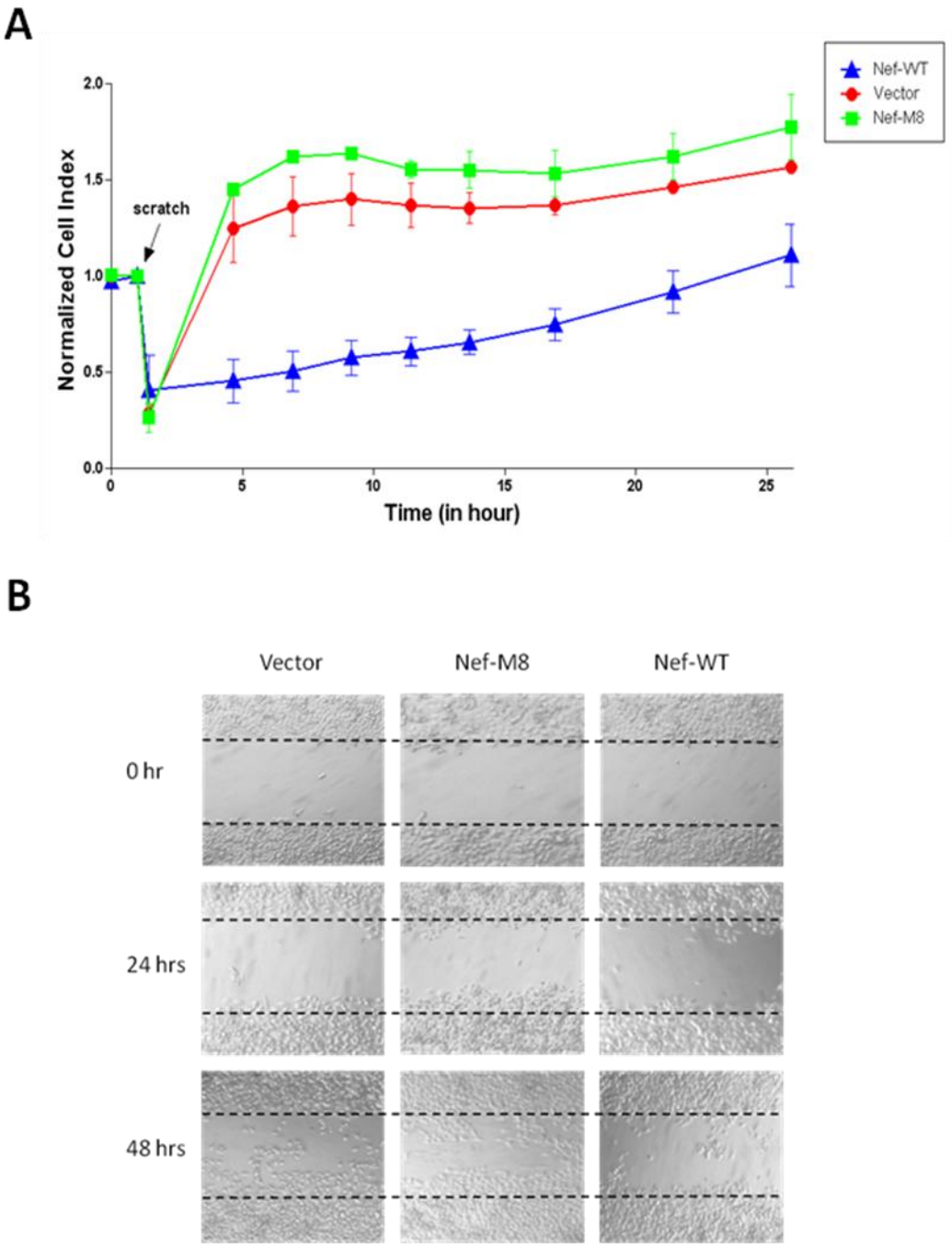

Figure 16. Nef from SIV_{mac239} inhibits migration of $HeLa\text{-}_{ACC}$ cells. A) Real-time cellular analysis reveals a quick increase of electric impedance after scratching Nef-M8 and vector control, but not Nef-WT transfected $HeLa\text{-}_{ACC}$ cells. **B)** Microscopical analysis shows cells migrating into the cell free scratched surface area. Nef-WT transfected $HeLa\text{-}_{ACC}$ cells exhibit reduced migratory abilities compared to control cells.

4.6 Effects of SIV_{mac239}-Nef on $CXCR4^+$ tumor cell invasiveness

Five x 10^5 Nef-WT, Nef-M8 and vector-only transfected HeLa-$_{ACC}$ cells, as well as untreated HeLa-$_{ACC}$ cells were applied on top of the MDCK monolayer. A7 melanoma cells served as a positive control whereas MDCK cells were used as a negative control. The electric resistance was measured over the following days (Fig. 17A). A reduction in TEER was observed in A7 melanoma cells within 3 days, whereas no obvious TEER was seen in the MDCK cells. Nef-WT transfected cells didn't show a reduction of TEER compared with Nef-M8 and vector-only control indicating that the Nef protein has no effect on invasiveness of HeLa-$_{ACC}$ cells in this specific assay.

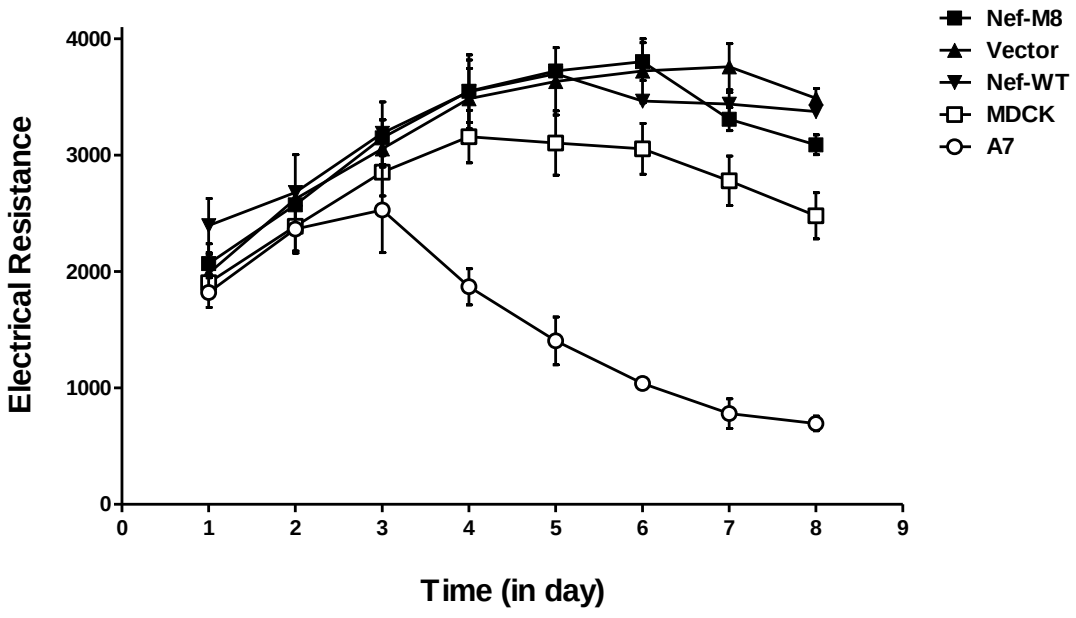

Figure 17A. Transepithelial electrical resistance breakdown (TEER) assay. SIV_{mac239}-Nef transfected HeLa-$_{ACC}$ cells did not exhibit enhanced invasiveness compared to control cells.

A similar result was also observed in a transwell invasion assay. No significant reduction of invasiveness can be detected in Nef-WT and CXCR4 siRNA transfected HeLa-$_{ACC}$ cells compared with vector-only (not shown), Nef-M8 or scrambled RNA transfected cells (Fig.17B).

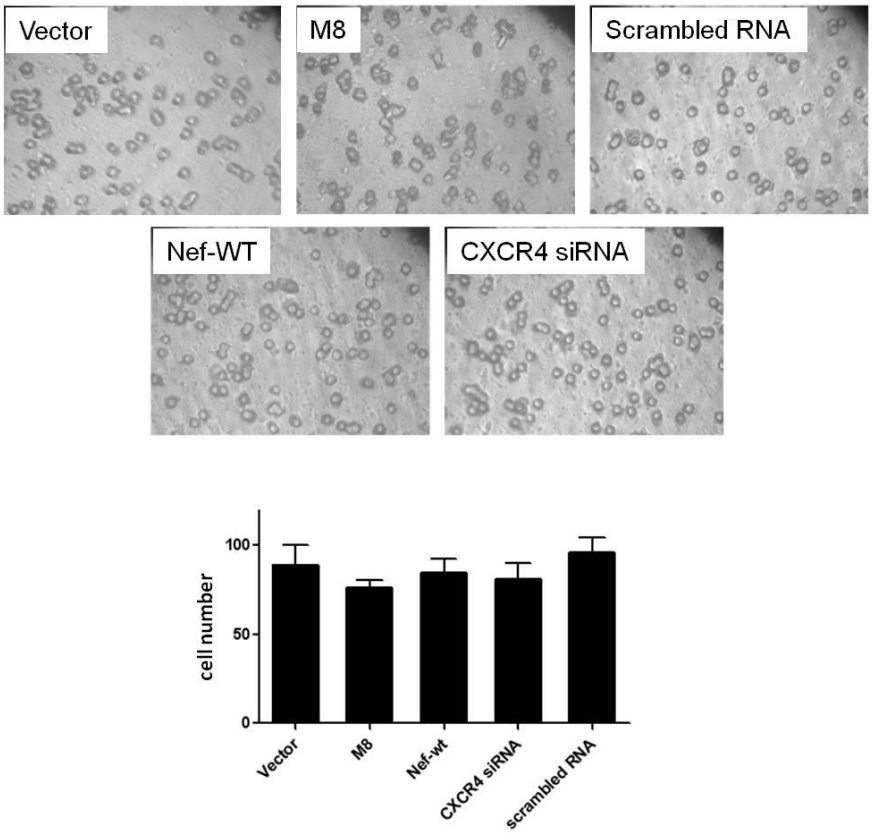

Figure 17B. Transwell invasion assay. No significant reduction of invasiveness can be observed in Nef-WT and CXCR4 siRNA transfeceted cells compared with M8, scrambled RNA or vector transfected cells.

4.7 *In vitro* tube formation of endothelial cells is reduced after transfection with SIV_{mac239}-Nef

In order to evaluate if SIV-Nef has an effect on angiogenesis, HUVEC cells were transfected with Nef-WT and CXCR4 siRNA. Untreated, Nef-M8, vector only or scrambled siRNA transfected cells were used as a negative control. Their tube formation abilities were evaluated by an *in vitro* tube formation assay as described above. Nef-WT transfected HUVEC cells, as well as CXCR4 siRNA transfected cells, demonstrated an inhibition of tube formation compared with Nef-M8 transfected cells (Fig. 18). Nef-M8 transfected HUVEC cells formed capillary structures similarly to untransfected and vector only transfected control cells (not shown).

HUVEC cells were also transfected with the two CXCR4 variants (CXCR4-Lo, CXCR4). Interestingly, CXCR4 over expression in HUVEC cells resulted in loss of most of its *in vitro* tube formation ability, whereas tube formation appeared similar between Nef-M8 control and CXCR4-Lo transfected HUVEC cells (Fig. 18).

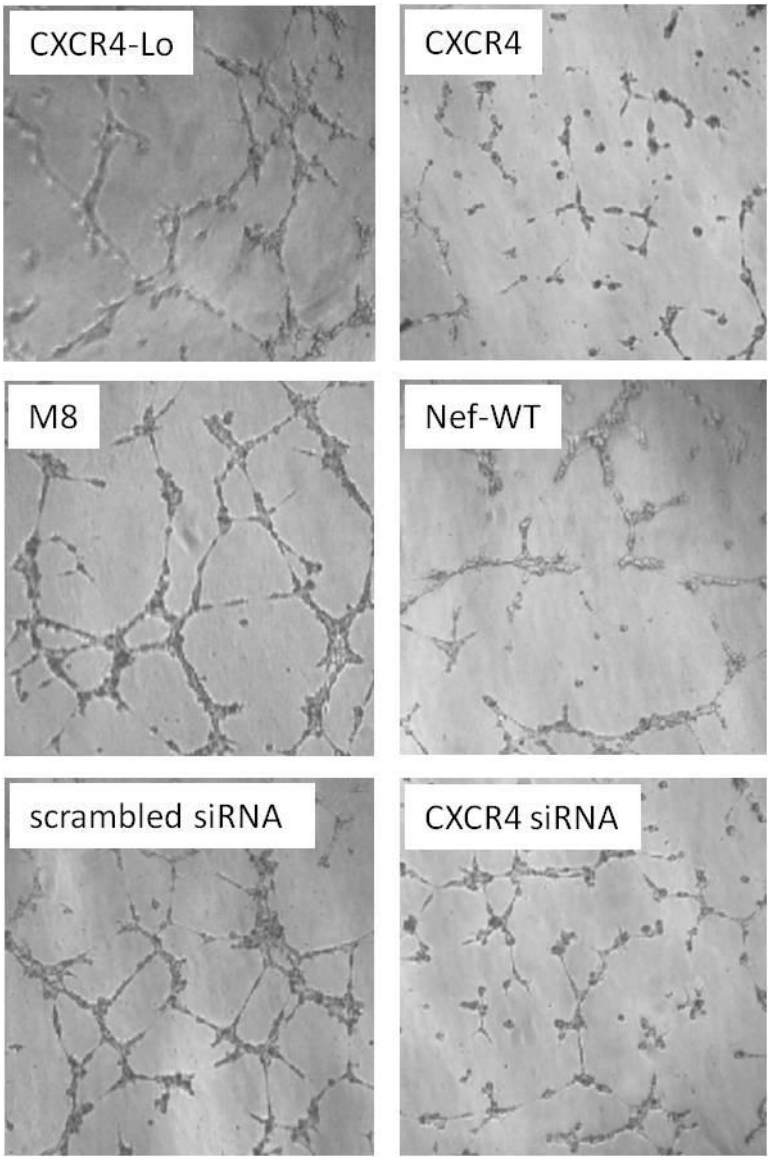

Figure 18. Nef inhibits angiogenesis. Nef-WT transfected HUVEC cells lost most of their *in vitro* tube formation ability compared with control cells (M8). A similar effect is observed after CXCR4 knockdown with siRNA. Overexpression of CXCR4 in HUVEC cells also inhibits tube formation.

4.8 SIV_{mac239}-Nef affects SDF-1α/CXCR4 signaling in $CXCR4^+$ tumor cells

The MAPK/ERK pathway is activated by the SDF-1/CXCR4 axis, which communicates signals from cell surface to the nucleus to activate transcription of genes involved in the regulation of chemotaxis, proliferation or apoptosis. To determine whether SIV-Nef has an effect on the MAPK/ERK pathway in tumor cells, Nef-WT transfected HeLa-$_{ACC}$ cells were treated with SDF-1α (100ng/ml). Cells were lysed 0, 5, 10 and 30min after incubation with the CXCR4 ligand. Phospho-STAT3, phosphorylated ERK1/2 and procaspase-3 cleavage were evaluated by Western blot analysis. Beta-actin was used as an internal control.

Higher levels of phospho-ERK1/2 were detected in Nef-WT transfected HeLa-$_{ACC}$ cells, which declined following treatment with SDF-1α. On the contrary, increased expression levels of phospho-ERK1/2 were detected in vector-only (Fig. 19) as well as Nef-M8 (data not shown) transfected cells. However, this effect was not pronounced.

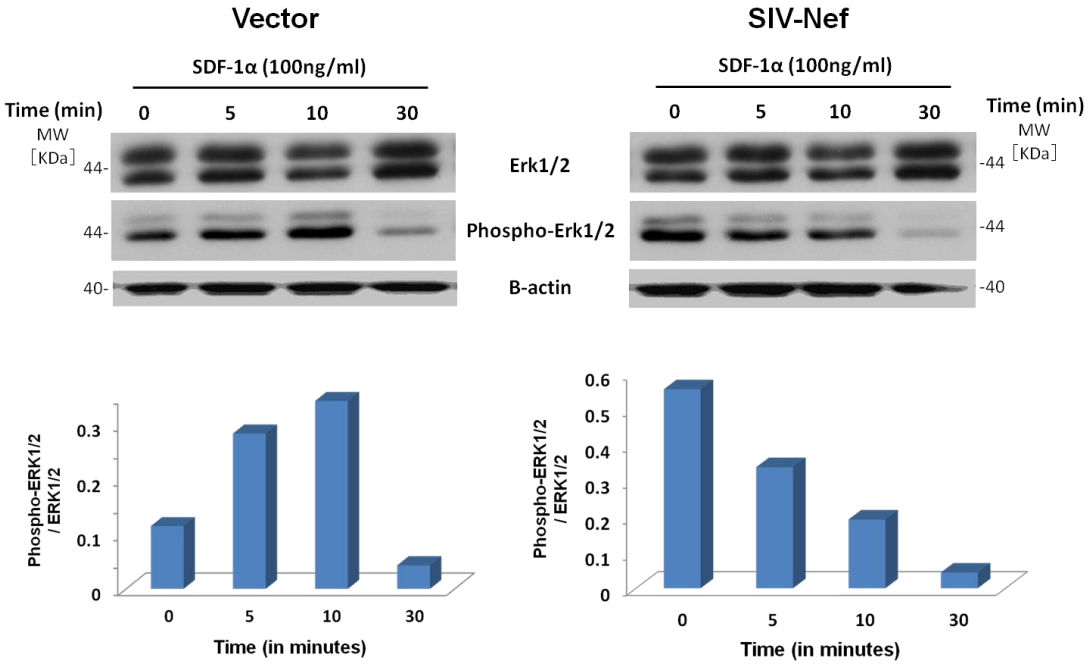

Figure 19. SIV-Nef inhibits MAPK/ERK signaling.

Compared with vector-only transfected control cells, a sharp decrease in STAT3 phosphorylation at 10min was detectable in Nef-WT transfected cells indicating that SIV-Nef affected phosphorylation of STAT3 (Fig. 20). No effect on procaspase-3 cleavage could be observed in Nef expressing and vector-only control cells, whereas cyclin-D1 was inhibited after transfection with Nef (Fig. 21). β-actin was used as an internal control.

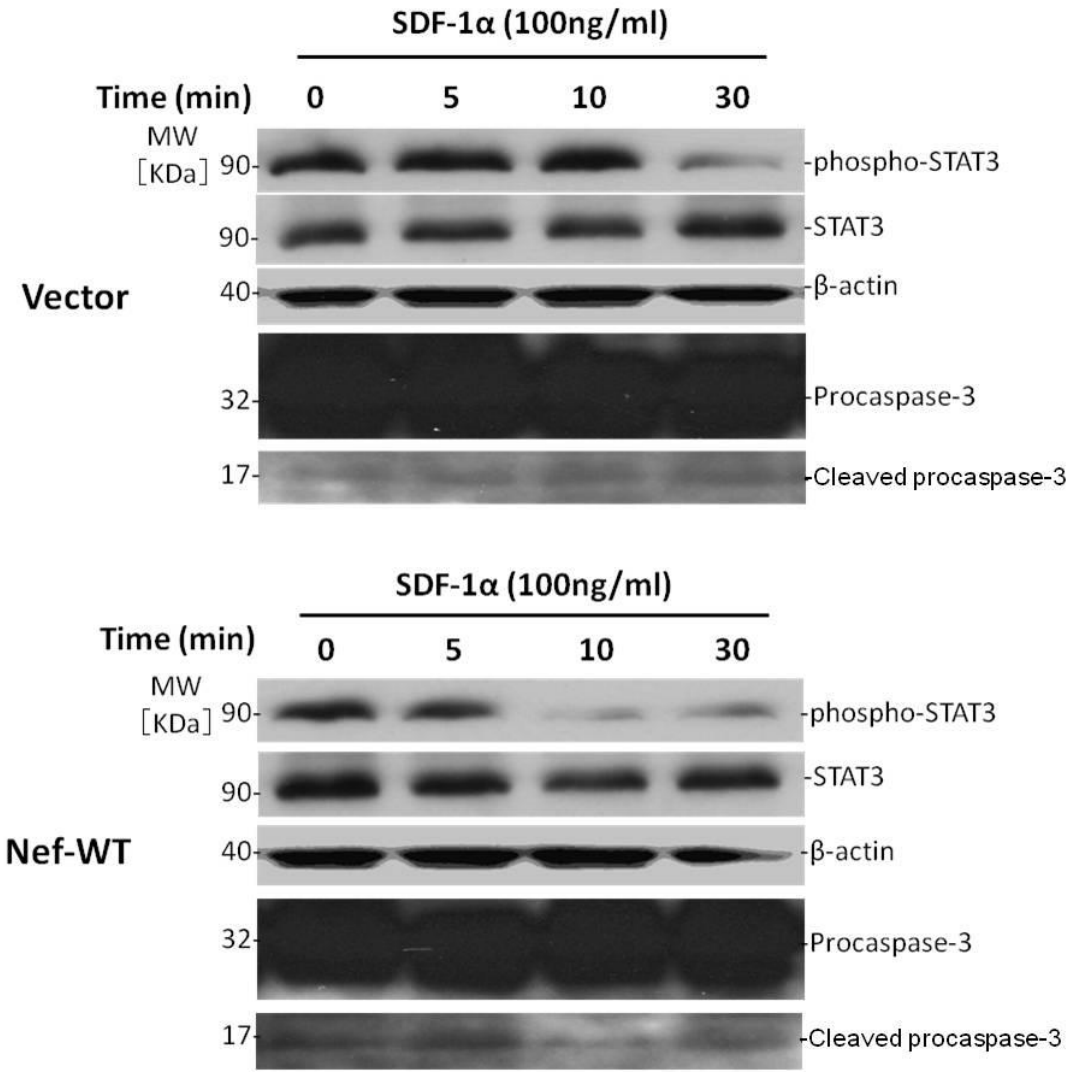

Figure 20. Enhanced inhibition of phospho-STAT3 in Nef-WT transfected HeLa-$_{ACC}$ cells. The expression of phospho-STAT3 in Nef transfected tumor cells was decreased after 10 min of treatment with SDF-1α, whereas the same reduction was visible 30 min after ligand treatment in control cells. No procaspase-3 cleavage was detectable in both vector and Nef transfected cells.

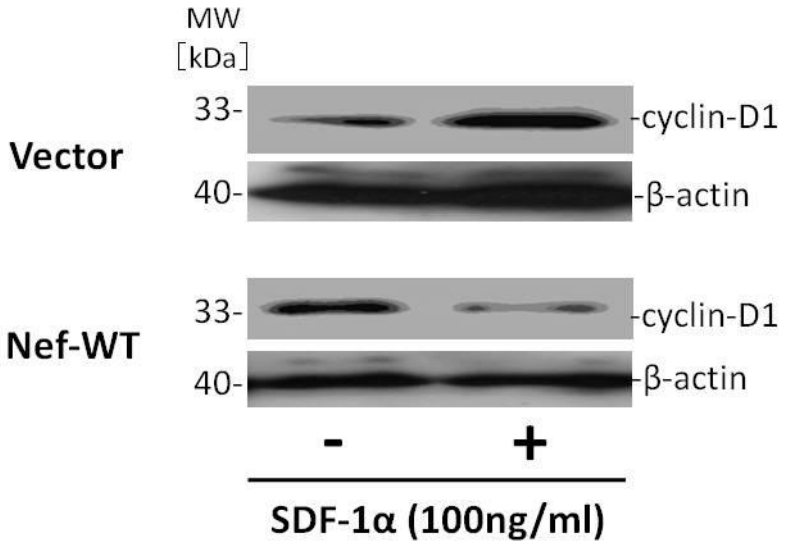

Figure 21. Cyclin-D1 is decreased in Nef transfected HeLa-$_{ACC}$ cells.

5. Discussion

Nef is a 27 kDa, N-terminal myristoylated HIV/SIV accessory protein. During the process of infection with HIV/SIV, Nef is down modulating MHC class I molecules from the cell surface of infected cells, is reducing MHC class II levels in antigen presenting cells (APCs) and CD8 levels in cytotoxic T lymphocytes [13;29;85;87] thereby promoting immune escape of the virus [20;22]. Nef also down regulates cell surface CXCR4, a major co-receptor of CD4, which is required for virus entry, to prevent lethal viral superinfection of the infected cell [29;58;94]. CXCR4 not only is known as a co-receptor for HIV/SIV entry but is also involved in malignant transformation, proliferation, migration and metastasis. It plays an important role in directing metastatic $CXCR4^+$ cells to organs that express high SDF-1α levels [53;67-69;106]. Therefore, targeting the CXCR4 receptor, e.g. with a CXCR4 inhibiting peptide such as ALX40-4C, is used as a therapeutic approach to prevent HIV/SIV infection as well as tumor metastasis [3;24].

In the present study wild-type Nef from SIV_{mac239}, which previously was shown to exhibit a potent down-modulating effect on CXCR4 in Jurkat T cells, was used to transfect CXCR4 positive tumor cells (HeLa-$_{ACC}$) to investigate if this viral protein also affects CXCR4 levels and related tumor relevant parameters such as proliferation, invasion and migration.

In HeLa-$_{ACC}$ cells, CXCR4 was found located at the plasma membrane as well as in the cytoplasm and nucleus. This is in accordance with previous reports that found a correlation of cytoplasmic and nuclear CXCR4 expression with lymph node metastasis and reduced overall survival in breast cancer and non-small cell lung cancer patients [70;102]. One explanation for the observed high level of intracellular CXCR4 could be a concomitant expression of SDF-1α since autocrine secretion of the ligand could result in enhanced endocytosis of the receptor with subsequent cytoplasmic and nuclear localization. Indeed,

co-expression of CXCR4 and SDF-1α was found to predict lymph node metastasis in colorectal cancer [103].

Transfection of HeLa-$_{ACC}$ cells with Nef resulted in down-regulation of CXCR4 from the cell surface, however, without markedly influencing CXCR4 total protein expression. Real-time cellular analysis of Nef transfected cells revealed that tumor cells transfected with the viral protein had a significantly reduced proliferation and migration rate. Recently, it was found that CXCR4 is closely involved in tumor angiogenesis. *In vitro* tube formation analysis displayed that HUVEC cells transfected with SIV-Nef partly lost their tube formation ability which not only indicated the important role of CXCR4 in angiogenesis but also a potential role of SIV-Nef for inhibition of tumor angiogenesis.

CXCR4/SDF-1α activates numerous intracellular signaling pathways to regulate cellular chemotaxis, migration, proliferation, apoptosis and adhesion. The MAPK/ERK pathway is the main signaling pathway stimulated by the activation of CXCR4/SDF-1α [41;56;84;90]. ERK can phosphorylate and activate downstream cellular protein, such as STAT3 [43;49;54;99], leading to changes in gene expression and cell cycle progress. ERK was found relatively inhibited in SIV-Nef expressing HeLa-$_{ACC}$ cells in response to the treatment of SDF-1α compared with Nef absent cells. STAT3, located downstream of ERK, was found markedly inhibited pointing to an influence of Nef on the MAPK/ERK pathway. Since activation of STAT3 is related to proliferation, cyclin-D1 expression was evaluated by Western blot analysis. Cyclin-D1 was found reduced in SIV-Nef expressing HeLa-$_{ACC}$ cells. Therefore, SIV-Nef could inhibit HeLa-$_{ACC}$ cell proliferation by a delay in cell cycle progression. This result is in accordance with a similar observation in CD4+ T cells [71]. No signs of apoptosis such as cleavage of procaspase-3 could be observed in any of the Nef-transfected cells (Fig.10; Fig.20) thereby not confirming that the SIV-Nef inhibiting effect exerted on HeLa-$_{ACC}$ cells is necessarily related to

programmed cell death as previously reported for HIV-1 Nef in Jurkat cells [60]. Nef affects intracellular signaling through a complex, not fully understood mechanism. STAT3 was phosphorylated or activated from a crosstalk way such as mTOR or JAKs. ERK was reportedly increased and PI3K was inhibited by HIV-Nef in Jurkat T cells as well as primary peripheral CD4+ T lymphocytes [16]. The effect of Nef on intracellular signaling is a subject for further studies.

Wild type but not mutated HIV-1-Nef was previously found to induce apoptosis in Jurkat T cells [6]. Subsequent mapping of Nef could reveal two specific regions (motifs) in the HIV-1-Nef sequence that exert apoptosis, with motif 1 (M1) being the most powerful one [42]. Interestingly, in a recent article this group used a Nef peptide (Nef-M1) representing the pro-apoptotic motif 1 to treat four colorectal cancer cell lines as well as colorectal xenografts in SCID mice. Here, they could observe a potent anti-tumor effect and concluded that the interaction of the Nef-M1 peptide with CXCR4 is responsible for the observed effect [38]. However, no obvious sequence similarities with these two HIV-Nef apoptosis inducing motifs can be found in SIV_{mac239}-Nef.

Motifs in the N-terminus and C-terminal flexible loop of SIV_{mac239}-Nef were found to be important for internalization of the viral protein [58]. In our study, the mutation Y28A (at the N-terminus) and $DE_{184}AA$, $LM_{194}AA$, $DD_{204}AA$ (in the C-terminal flexible loop) lead to a reduction of cellular proliferation, indicating that these motifs in SIV-Nef play a role in regulating cell surface CXCR4 and tumor cell proliferation.

CXCR4-Lo is a transcript variant of CXCR4, which contains a longer N-terminus when compared to CXCR4. CXCR4-Lo reportedly could be a competitor of CXCR4 for its binding to SDF-1α. Few studies focused on CXCR4-Lo since its discovery in 1999 [36]. Its function relative to CXCR4 remains unclear. In order to better understand if CXCR4-Lo is also sensitive to SIV-Nef down regulation, CXCR4-Lo was expressed in COS-7 cells. CXCR4-Lo localized to the cell membrane, cytoplasm and even the nucleus in

RFP-CXCR4-Lo transfected COS-7 cells similarly as observed for CXCR4. SIV-Nef could down regulate cell surface CXCR4-Lo but as it appears to a smaller extent than CXCR4. Influence on proliferation in CXCR4-Lo transfected HeLa-$_{ACC}$ cells was not obvious (data not shown). The data indicates that CXCR4 could play a major role in SIV-Nef mediated inhibition of tumor cell proliferation and migration. Interestingly, CXCR4 overexpressing HUVEC cells showed a reduction of *in vitro* tube formation ability. The transfection of one of the CXCR4 isoforms potentially could break the balance between the two variants thereby affecting angiogenesis. The mechanism behind this effect is currently unknown and subject to ongoing studies.

Since CXCR4/SDF-1α plays such an important role in tumor growth, many anti-SDF-1α or anti-CXCR4 directed agents such as AMD3100, NOX-A12 or CCX2066 were developed and used in preclinical *in vivo* studies partly demonstrating a significant decrease in tumor growth [14;44;72;81]. Our data indicate that Nef from SIV$_{mac239}$ can down-modulate plasma membrane associated CXCR4 in CXCR4^{+} tumor cells and that expression of the viral protein could further result in reduction of tumor cell proliferation, migration and angiogenesis. SIV-Nef therefore could serve as an interesting experimental tool for the study of CXCR4-expressing tumors and potentially could help to pinpoint new therapeutic approaches for the treatment of these malignancies.

6. Summary

The HIV/SIV accessory protein Nef is known to down-modulate cell surface receptors that are required for virus entry such as CD4, CCR5 and CXCR4 to block lethal viral superinfection of the infected cell. The chemokine receptor CXCR4 also plays an important role in promoting tumor cell proliferation, metastasis and angiogenesis. Therefore it was of interest to evaluate if Nef can down-regulate CXCR4 in tumor cells since this could affect these critical prognostic parameters. The $CXCR4^+$ tumor cell line HeLa-$_{ACC}$ was transfected with Nef from SIV_{mac239} and cell surface expression of the receptor was monitored by FACS analysis. Real-time cellular analysis was performed and cell migration was evaluated by an *in vitro* scratch assay. The *in vitro* tube formation assay was carried out on Nef transfected HUVEC cells to evaluate if Nef affects angiogenesis. Also, the influence of Nef on intracellular signaling was evaluated by Western blot analysis. Additionally, COS-7 cells were co-transfected with Nef and CXCR4 or its transcript variant, CXCR4-Lo, and were treated in the same way as described for HeLa-$_{ACC}$.

In this study, cell surface down-modulation of endogenous CXCR4 could be observed in HeLa-$_{ACC}$ cells after Nef-transfection as well as in COS-7 cells after co-transfection of CXCR4 and Nef. Proliferation as well as migration of Nef-transfected HeLa-$_{ACC}$ tumor cells was significantly reduced. Nef transfected HUVEC cells lost most of their tube formation ability. The CXCR4 transcript variant, CXCR4-Lo, could also be down-regulated by Nef in COS-7 cells. Interestingly, a reduced tube formation ability was observed in CXCR4 overexpressed HUVEC cells, whereas CXCR4-Lo transfected HUVEC cells displayed similar tube formation levels compared to the vector control transfected cells.

Our data demonstrated that Nef from SIV_{mac239} can down-modulate plasma membrane associated CXCR4 in a $CXCR4^+$ tumor cell line (HeLa-$_{ACC}$). Transfection of HeLa-$_{ACC}$ or HUVEC cells resulted in reduction of tumor cell

proliferation, migration and angiogenesis. SIV-Nef therefore could serve as an interesting experimental tool for the study of CXCR4-expressing tumors and potentially could help to pinpoint new therapeutic approaches for the treatment of these malignancies.

7. Reference

[1] A. Adachi, Y. Oshima, Cell-dependent functional roles of HIV-1 Nef for virus replication (review). Int.J.Mol.Med. 3 (1999) 427-430.

[2] B.Y. Alabyev, A.M. Najakshin, L.V. Mechetina, A.V. Taranin, Cloning of a CXCR4 homolog in chondrostean fish and characterization of the CXCR4-specific structural features. Dev.Comp Immunol. 24 (2000) 765-770.

[3] R.E. Bachelder, M.A. Wendt, A.M. Mercurio, Vascular endothelial growth factor promotes breast carcinoma invasion in an autocrine manner by regulating the chemokine receptor CXCR4. Cancer Res. 62 (2002) 7203-7206.

[4] F. Balkwill, Cancer and the chemokine network. Nat.Rev.Cancer 4 (2004) 540-550.

[5] F. Barbieri, A. Bajetto, R. Stumm, A. Pattarozzi, C. Porcile, G. Zona, A. Dorcaratto, J.L. Ravetti, F. Minuto, R. Spaziante, G. Schettini, D. Ferone, T. Florio, Overexpression of stromal cell-derived factor 1 and its receptor CXCR4 induces autocrine/paracrine cell proliferation in human pituitary adenomas. Clin.Cancer Res. 14 (2008) 5022-5032.

[6] A.S. Baur, E.T. Sawai, P. Dazin, W.J. Fantl, C. Cheng-Mayer, B.M. Peterlin, HIV-1 Nef leads to inhibition or activation of T cells depending on its intracellular localization. Immunity. 1 (1994) 373-384.

[7] I. Bell, T.M. Schaefer, R.P. Trible, A. Amedee, T.A. Reinhart, Down-modulation of the costimulatory molecule, CD28, is a conserved activity of multiple SIV Nefs and is dependent on histidine 196 of Nef. Virology 283 (2001) 148-158.

[8] M. Bentham, S. Mazaleyrat, M. Harris, Role of myristoylation and N-terminal basic residues in membrane association of the human immunodeficiency virus type 1 Nef protein. J.Gen.Virol. 87 (2006) 563-571.

[9] A.D. Blagoveshchenskaya, L. Thomas, S.F. Feliciangeli, C.H. Hung, G. Thomas, HIV-1

Nef downregulates MHC-I by a PACS-1- and PI3K-regulated ARF6 endocytic pathway. Cell 111 (2002) 853-866.

[10] M. Brenner, J. Munch, M. Schindler, S. Wildum, N. Stolte, C. Stahl-Hennig, D. Fuchs, K. Matz-Rensing, M. Franz, J. Heeney, H.P. Ten, T. Swigut, K. Hrecka, J. Skowronski, F. Kirchhoff, Importance of the N-distal AP-2 binding element in Nef for simian immunodeficiency virus replication and pathogenicity in rhesus macaques. J.Virol. 80 (2006) 4469-4481.

[11] X. Carnec, L. Quan, W.C. Olson, U. Hazan, T. Dragic, Anti-CXCR4 monoclonal antibodies recognizing overlapping epitopes differ significantly in their ability to inhibit entry of human immunodeficiency virus type 1. J Virol. 79 (2005) 1930-1933.

[12] H.Y. Chang, H. Nishitoh, X. Yang, H. Ichijo, D. Baltimore, Activation of apoptosis signal-regulating kinase 1 (ASK1) by the adapter protein Daxx. Science 281 (1998) 1860-1863.

[13] A. Chaudhry, D.A. Verghese, S.R. Das, S. Jameel, A. George, V. Bal, S. Mayor, S. Rath, HIV-1 Nef promotes endocytosis of cell surface MHC class II molecules via a constitutive pathway. J.Immunol. 183 (2009) 2415-2424.

[14] X.P. Chen, L.L. Qian, H. Jiang, J.H. Chen, Ginsenoside Rg3 inhibits CXCR(4) expression and related migrations in a breast cancer cell line. Int.J.Clin.Oncol.2011).

[15] J. Cheng, T. Irie, R. Munakata, S. Kimura, H. Nakamura, R.G. He, A.R. Lui, T. Saku, Biosynthesis of basement membrane molecules by salivary adenoid cystic carcinoma cells: an immunofluorescence and confocal microscopic study. Virchows Arch. 426 (1995) 577-586.

[16] E.Y. Choe, E.S. Schoenberger, J.E. Groopman, I.W. Park, HIV Nef inhibits T cell migration. J.Biol.Chem. 277 (2002) 46079-46084.

[17] H. Choe, Chemokine receptors in HIV-1 and SIV infection. Arch.Pharm.Res. 21 (1998)

634-639.

[18] H. Choe, K.A. Martin, M. Farzan, J. Sodroski, N.P. Gerard, C. Gerard, Structural interactions between chemokine receptors, gp120 Env and CD4. Semin.Immunol. 10 (1998) 249-257.

[19] M.Y. Chowers, C.A. Spina, T.J. Kwoh, N.J. Fitch, D.D. Richman, J.C. Guatelli, Optimal infectivity in vitro of human immunodeficiency virus type 1 requires an intact nef gene. J.Virol. 68 (1994) 2906-2914.

[20] K.L. Collins, B.K. Chen, S.A. Kalams, B.D. Walker, D. Baltimore, HIV-1 Nef protein protects infected primary cells against killing by cytotoxic T lymphocytes. Nature 391 (1998) 397-401.

[21] F. Corpet, Multiple sequence alignment with hierarchical clustering. Nucleic Acids Res. 16 (1988) 10881-10890.

[22] R.W. Doms, D. Trono, The plasma membrane as a combat zone in the HIV battlefield. Genes Dev. 14 (2000) 2677-2688.

[23] X. Dong, P. Stothard, I.J. Forsythe, D.S. Wishart, PlasMapper: a web server for drawing and auto-annotating plasmid maps. Nucleic Acids Res. 32 (2004) W660-W664.

[24] B.J. Doranz, L.G. Filion, F. az-Mitoma, D.S. Sitar, J. Sahai, F. Baribaud, M.J. Orsini, J.L. Benovic, W. Cameron, R.W. Doms, Safe use of the CXCR4 inhibitor ALX40-4C in humans. AIDS Res.Hum.Retroviruses 17 (2001) 475-486.

[25] B.J. Doranz, M.J. Orsini, J.D. Turner, T.L. Hoffman, J.F. Berson, J.A. Hoxie, S.C. Peiper, L.F. Brass, R.W. Doms, Identification of CXCR4 domains that support coreceptor and chemokine receptor functions. J.Virol. 73 (1999) 2752-2761.

[26] E.J. Fernandez, E. Lolis, Structure, function, and inhibition of chemokines.

Annu.Rev.Pharmacol.Toxicol. 42 (2002) 469-499.

[27] A.D. Frankel, J.A. Young, HIV-1: fifteen proteins and an RNA. Annu.Rev.Biochem. 67 (1998) 1-25.

[28] R.K. Ganju, S.A. Brubaker, J. Meyer, P. Dutt, Y. Yang, S. Qin, W. Newman, J.E. Groopman, The alpha-chemokine, stromal cell-derived factor-1alpha, binds to the transmembrane G-protein-coupled CXCR-4 receptor and activates multiple signal transduction pathways. J.Biol.Chem. 273 (1998) 23169-23175.

[29] J.V. Garcia, A.D. Miller, Serine phosphorylation-independent downregulation of cell-surface CD4 by nef. Nature 350 (1991) 508-511.

[30] P. Gassmann, J. Haier, K. Schluter, B. Domikowsky, C. Wendel, U. Wiesner, R. Kubitza, R. Engers, S.W. Schneider, B. Homey, A. Muller, CXCR4 regulates the early extravasation of metastatic tumor cells in vivo. Neoplasia. 11 (2009) 651-661.

[31] R. Geleziunas, W. Xu, K. Takeda, H. Ichijo, W.C. Greene, HIV-1 Nef inhibits ASK1-dependent death signalling providing a potential mechanism for protecting the infected host cell. Nature 410 (2001) 834-838.

[32] Y. Gluzman, SV40-transformed simian cells support the replication of early SV40 mutants. Cell 23 (1981) 175-182.

[33] M.E. Greenberg, A.J. Iafrate, J. Skowronski, The SH3 domain-binding surface and an acidic motif in HIV-1 Nef regulate trafficking of class I MHC complexes. EMBO J. 17 (1998) 2777-2789.

[34] A.L. Greenway, D.A. McPhee, K. Allen, R. Johnstone, G. Holloway, J. Mills, A. Azad, S. Sankovich, P. Lambert, Human immunodeficiency virus type 1 Nef binds to tumor suppressor p53 and protects cells against p53-mediated apoptosis. J.Virol. 76 (2002) 2692-2702.

[35] A. Gross, J.M. McDonnell, S.J. Korsmeyer, BCL-2 family members and the mitochondria in apoptosis. Genes Dev. 13 (1999) 1899-1911.

[36] S.K. Gupta, K. Pillarisetti, Cutting edge: CXCR4-Lo: molecular cloning and functional expression of a novel human CXCR4 splice variant. J.Immunol. 163 (1999) 2368-2372.

[37] B. Guy, M.P. Kieny, Y. Riviere, P.C. Le, K. Dott, M. Girard, L. Montagnier, J.P. Lecocq, HIV F/3' orf encodes a phosphorylated GTP-binding protein resembling an oncogene product. Nature 330 (1987) 266-269.

[38] W. Harrington, V. Bond, M.B. Huang, M. Powell, J. Lillard, U. Manne, H. Bumpers, HIV Nef-M1 Effects on Colorectal Cancer Growth in Tumor-induced Spleens and Hepatic Metastasis. Mol.Cell Pharmacol. 1 (2009) 85-91.

[39] He RG, Z.X.W.Z.Z.X.Q.W.H.Y.Z.R. Zhang XS. The establishment of cell lines of adenoid cystic carcinoma of human salivary glands (ACC2, ACC3) and a study of morphology. West Chin J Stomatol 6, 1-4. 1988. Ref Type: Generic

[40] K. Hrecka, T. Swigut, M. Schindler, F. Kirchhoff, J. Skowronski, Nef proteins from diverse groups of primate lentiviruses downmodulate CXCR4 to inhibit migration to the chemokine stromal derived factor 1. J.Virol. 79 (2005) 10650-10659.

[41] C.Y. Huang, C.Y. Lee, M.Y. Chen, W.H. Yang, Y.H. Chen, C.H. Chang, H.C. Hsu, Y.C. Fong, C.H. Tang, Stromal cell-derived factor-1/CXCR4 enhanced motility of human osteosarcoma cells involves MEK1/2, ERK and NF-kappaB-dependent pathways. J.Cell Physiol 221 (2009) 204-212.

[42] M.B. Huang, L.L. Jin, C.O. James, M. Khan, M.D. Powell, V.C. Bond, Characterization of Nef-CXCR4 interactions important for apoptosis induction. J.Virol. 78 (2004) 11084-11096.

[43] N. Jain, T. Zhang, S.L. Fong, C.P. Lim, X. Cao, Repression of Stat3 activity by

activation of mitogen-activated protein kinase (MAPK). Oncogene 17 (1998) 3157-3167.

[44] A. Kawaguchi, Y. Orba, T. Kimura, H. Iha, M. Ogata, T. Tsuji, A. Ainai, T. Sata, T. Okamoto, W.W. Hall, H. Sawa, H. Hasegawa, Inhibition of the SDF-1alpha-CXCR4 axis by the CXCR4 antagonist AMD3100 suppresses the migration of cultured cells from ATL patients and murine lymphoblastoid cells from HTLV-I Tax transgenic mice. Blood 114 (2009) 2961-2968.

[45] J. Kimpton, M. Emerman, Detection of replication-competent and pseudotyped human immunodeficiency virus with a sensitive cell line on the basis of activation of an integrated beta-galactosidase gene. J.Virol. 66 (1992) 2232-2239.

[46] R. Klein, D. Conway, L.F. Parada, M. Barbacid, The trkB tyrosine protein kinase gene codes for a second neurogenic receptor that lacks the catalytic kinase domain. Cell 61 (1990) 647-656.

[47] M.E. Klotman, S. Kim, A. Buchbinder, A. DeRossi, D. Baltimore, F. Wong-Staal, Kinetics of expression of multiply spliced RNA in early human immunodeficiency virus type 1 infection of lymphocytes and monocytes. Proc.Natl.Acad.Sci.U.S.A 88 (1991) 5011-5015.

[48] I. Kryczek, S. Wei, E. Keller, R. Liu, W. Zou, Stroma-derived factor (SDF-1/CXCL12) and human tumor pathogenesis. Am.J.Physiol Cell Physiol 292 (2007) C987-C995.

[49] M. Kuroki, J.T. O'Flaherty, Extracellular signal-regulated protein kinase (ERK)-dependent and ERK-independent pathways target STAT3 on serine-727 in human neutrophils stimulated by chemotactic factors and cytokines. Biochem.J 341 (Pt 3) (1999) 691-696.

[50] K.J. Laing, C.J. Secombes, Chemokines. Dev.Comp Immunol. 28 (2004) 443-460.

[51] G.S. Le, L. Erdtmann, S. Benichou, C. Berlioz-Torrent, L. Liu, R. Benarous, J.M. Heard,

O. Schwartz, Nef interacts with the mu subunit of clathrin adaptor complexes and reveals a cryptic sorting signal in MHC I molecules. Immunity. 8 (1998) 483-495.

[52] C.C. Liang, A.Y. Park, J.L. Guan, In vitro scratch assay: a convenient and inexpensive method for analysis of cell migration in vitro. Nat.Protoc. 2 (2007) 329-333.

[53] L.A. Liotta, An attractive force in metastasis. Nature 410 (2001) 24-25.

[54] R.K. Lo, H. Cheung, Y.H. Wong, Constitutively active Galpha16 stimulates STAT3 via a c-Src/JAK- and ERK-dependent mechanism. J Biol.Chem. 278 (2003) 52154-52165.

[55] X. Lu, H. Yu, S.H. Liu, F.M. Brodsky, B.M. Peterlin, Interactions between HIV1 Nef and vacuolar ATPase facilitate the internalization of CD4. Immunity. 8 (1998) 647-656.

[56] Y. Luo, J. Lathia, M. Mughal, M.P. Mattson, SDF1alpha/CXCR4 signaling, via ERKs and the transcription factor Egr1, induces expression of a 67-kDa form of glutamic acid decarboxylase in embryonic hippocampal neurons. J.Biol.Chem. 283 (2008) 24789-24800.

[57] Q. Ma, D. Jones, P.R. Borghesani, R.A. Segal, T. Nagasawa, T. Kishimoto, R.T. Bronson, T.A. Springer, Impaired B-lymphopoiesis, myelopoiesis, and derailed cerebellar neuron migration in C. Proc.Natl.Acad.Sci.U.S.A 95 (1998) 9448-9453.

[58] R. Mandic, O.T. Fackler, M. Geyer, T. Linnemann, Y.H. Zheng, B.M. Peterlin, Negative factor from SIV binds to the catalytic subunit of the V-ATPase to internalize CD4 and to increase viral infectivity. Mol.Biol.Cell 12 (2001) 463-473.

[59] R. Mandic, T. Ludwig, H. Oberleithner, J.A. Werner, Evaluation of head and neck squamous cell carcinoma invasiveness by the electrical resistance breakdown assay. Clin.Exp.Metastasis 21 (2004) 699-704.

[60] R. Mandic, C.J. Schamberger, J.F. Muller, M. Geyer, L. Zhu, T.E. Carey, R. Grenman, A.A. Dunne, J.A. Werner, Reduced cisplatin sensitivity of head and neck squamous

cell carcinoma cell lines correlates with mutations affecting the COOH-terminal nuclear localization signal of p53. Clin.Cancer Res. 11 (2005) 6845-6852.

[61] D. Martin-Zanca, S.H. Hughes, M. Barbacid, A human oncogene formed by the fusion of truncated tropomyosin and protein tyrosine kinase sequences. Nature 319 (1986) 743-748.

[62] R. Meier, A. Muhlethaler-Mottet, M. Flahaut, A. Coulon, C. Fusco, F. Louache, K. Auderset, K.B. Bourloud, E. Daudigeos, C. Ruegg, G. Vassal, N. Gross, J.M. Joseph, The chemokine receptor CXCR4 strongly promotes neuroblastoma primary tumour and metastatic growth, but not invasion. PLoS.One. 2 (2007) e1016.

[63] M. Mellado, J.M. Rodriguez-Frade, S. Manes, A. Martinez, Chemokine signaling and functional responses: the role of receptor dimerization and TK pathway activation. Annu.Rev.Immunol. 19 (2001) 397-421.

[64] Z. Miao, K.E. Luker, B.C. Summers, R. Berahovich, M.S. Bhojani, A. Rehemtulla, C.G. Kleer, J.J. Essner, A. Nasevicius, G.D. Luker, M.C. Howard, T.J. Schall, CXCR7 (RDC1) promotes breast and lung tumor growth in vivo and is expressed on tumor-associated vasculature. Proc.Natl.Acad.Sci.U.S.A 104 (2007) 15735-15740.

[65] N. Michel, I. Allespach, S. Venzke, O.T. Fackler, O.T. Keppler, The Nef protein of human immunodeficiency virus establishes superinfection immunity by a dual strategy to downregulate cell-surface CCR5 and CD4. Curr.Biol. 15 (2005) 714-723.

[66] N. Michel, K. Ganter, S. Venzke, J. Bitzegeio, O.T. Fackler, O.T. Keppler, The Nef protein of human immunodeficiency virus is a broad-spectrum modulator of chemokine receptor cell surface levels that acts independently of classical motifs for receptor endocytosis and Galphai signaling. Mol.Biol.Cell 17 (2006) 3578-3590.

[67] A. Muller, B. Homey, H. Soto, N. Ge, D. Catron, M.E. Buchanan, T. McClanahan, E. Murphy, W. Yuan, S.N. Wagner, J.L. Barrera, A. Mohar, E. Verastegui, A. Zlotnik,

Involvement of chemokine receptors in breast cancer metastasis. Nature 410 (2001) 50-56.

[68] A. Muller, E. Sonkoly, C. Eulert, P.A. Gerber, R. Kubitza, K. Schirlau, P. Franken-Kunkel, C. Poremba, C. Snyderman, L.O. Klotz, T. Ruzicka, H. Bier, A. Zlotnik, T.L. Whiteside, B. Homey, T.K. Hoffmann, Chemokine receptors in head and neck cancer: association with metastatic spread and regulation during chemotherapy. Int.J.Cancer 118 (2006) 2147-2157.

[69] T. Murakami, W. Maki, A.R. Cardones, H. Fang, K.A. Tun, F.O. Nestle, S.T. Hwang, Expression of CXC chemokine receptor-4 enhances the pulmonary metastatic potential of murine B16 melanoma cells. Cancer Res. 62 (2002) 7328-7334.

[70] I.K. Na, C. Scheibenbogen, C. Adam, A. Stroux, P. Ghadjar, E. Thiel, U. Keilholz, S.E. Coupland, Nuclear expression of CXCR4 in tumor cells of non-small cell lung cancer is correlated with lymph node metastasis. Hum.Pathol. 39 (2008) 1751-1755.

[71] T. Ndolo, N.K. Dhillon, H. Nguyen, M. Guadalupe, M. Mudryj, S. Dandekar, Simian immunodeficiency virus Nef protein delays the progression of CD4+ T cells through G1/S phase of the cell cycle. J.Virol. 76 (2002) 3587-3595.

[72] S. Otsuka, G. Bebb, The CXCR4/SDF-1 chemokine receptor axis: a new target therapeutic for non-small cell lung cancer. J.Thorac.Oncol. 3 (2008) 1379-1383.

[73] S.M. Owen, S. Masciotra, F. Novembre, J. Yee, W.M. Switzer, M. Ostyula, R.B. Lal, Simian immunodeficiency viruses of diverse origin can use CXCR4 as a coreceptor for entry into human cells. J.Virol. 74 (2000) 5702-5708.

[74] I. Petit, D. Jin, S. Rafii, The SDF-1-CXCR4 signaling pathway: a molecular hub modulating neo-angiogenesis. Trends Immunol. 28 (2007) 299-307.

[75] J. Phuchareon, Y. Ohta, J.M. Woo, D.W. Eisele, O. Tetsu, Genetic profiling reveals cross-contamination and misidentification of 6 adenoid cystic carcinoma cell lines:

ACC2, ACC3, ACCM, ACCNS, ACCS and CAC2. PLoS.One. 4 (2009) e6040.

[76] V. Piguet, L. Wan, C. Borel, A. Mangasarian, N. Demaurex, G. Thomas, D. Trono, HIV-1 Nef protein binds to the cellular protein PACS-1 to downregulate class I major histocompatibility complexes. Nat.Cell Biol. 2 (2000) 163-167.

[77] N. Pore, A. Maity, The chemokine receptor CXCR4: a homing device for hypoxic cancer cells? Cancer Biol.Ther. 5 (2006) 1563-1565.

[78] A. Raney, A.Y. Shaw, J.L. Foster, J.V. Garcia, Structural constraints on human immunodeficiency virus type 1 Nef function. Virology 368 (2007) 7-16.

[79] M.Z. Ratajczak, E. Zuba-Surma, M. Kucia, R. Reca, W. Wojakowski, J. Ratajczak, The pleiotropic effects of the SDF-1-CXCR4 axis in organogenesis, regeneration and tumorigenesis. Leukemia 20 (2006) 1915-1924.

[80] M. Roshal, Y. Zhu, V. Planelles, Apoptosis in AIDS. Apoptosis. 6 (2001) 103-116.

[81] C. Rubie, V.O. Frick, P. Ghadjar, M. Wagner, C. Justinger, S.K. Faust, B. Vicinus, S. Graber, O. Kollmar, M.K. Schilling, CXC receptor-4 mRNA silencing abrogates CXCL12-induced migration of colorectal cancer cells. J.Transl.Med. 9 (2011) 22.

[82] M. Schindler, S. Wurfl, P. Benaroch, T.C. Greenough, R. Daniels, P. Easterbrook, M. Brenner, J. Munch, F. Kirchhoff, Down-modulation of mature major histocompatibility complex class II and up-regulation of invariant chain cell surface expression are well-conserved functions of human and simian immunodeficiency virus nef alleles. J.Virol. 77 (2003) 10548-10556.

[83] O. Schwartz, V. Marechal, G.S. Le, F. Lemonnier, J.M. Heard, Endocytosis of major histocompatibility complex class I molecules is induced by the HIV-1 Nef protein. Nat.Med. 2 (1996) 338-342.

[84] T.D. Southgate, O.J. McGinn, F.V. Castro, A.J. Rutkowski, M. Al-Muftah, G. Marinov,

G.J. Smethurst, D. Shaw, C.M. Ward, C.J. Miller, P.L. Stern, CXCR4 mediated chemotaxis is regulated by 5T4 oncofetal glycoprotein in mouse embryonic cells. PLoS.One. 5 (2010) e9982.

[85] V. Stove, d.W. Van, I, E. Naessens, E. Coene, C. Stove, J. Plum, B. Verhasselt, Human immunodeficiency virus Nef induces rapid internalization of the T-cell coreceptor CD8alphabeta. J.Virol. 79 (2005) 11422-11433.

[86] P. Stumptner-Cuvelette, M. Jouve, J. Helft, M. Dugast, A.S. Glouzman, K. Jooss, G. Raposo, P. Benaroch, Human immunodeficiency virus-1 Nef expression induces intracellular accumulation of multivesicular bodies and major histocompatibility complex class II complexes: potential role of phosphatidylinositol 3-kinase. Mol.Biol.Cell 14 (2003) 4857-4870.

[87] P. Stumptner-Cuvelette, S. Morchoisne, M. Dugast, G.S. Le, G. Raposo, O. Schwartz, P. Benaroch, HIV-1 Nef impairs MHC class II antigen presentation and surface expression. Proc.Natl.Acad.Sci.U.S.A 98 (2001) 12144-12149.

[88] B. Sung, S. Jhurani, K.S. Ahn, Y. Mastuo, T. Yi, S. Guha, M. Liu, B.B. Aggarwal, Zerumbone down-regulates chemokine receptor CXCR4 expression leading to inhibition of CXCL12-induced invasion of breast and pancreatic tumor cells. Cancer Res. 68 (2008) 8938-8944.

[89] T. Swigut, N. Shohdy, J. Skowronski, Mechanism for down-regulation of CD28 by Nef. EMBO J. 20 (2001) 1593-1604.

[90] C.H. Tang, J.Y. Chuang, Y.C. Fong, M.C. Maa, T.D. Way, C.H. Hung, Bone-derived SDF-1 stimulates IL-6 release via CXCR4, ERK and NF-kappaB pathways and promotes osteoclastogenesis in human oral cancer cells. Carcinogenesis 29 (2008) 1483-1492.

[91] B.A. Teicher, S.P. Fricker, CXCL12 (SDF-1)/CXCR4 pathway in cancer. Clin.Cancer

Res. 16 (2010) 2927-2931.

[92] K. Tokunaga, A. Kojima, T. Kurata, K. Ikuta, H. Akari, A.H. Koyama, M. Kawamura, R. Inubushi, R. Shimano, A. Adachi, Enhancement of human immunodeficiency virus type 1 infectivity by Nef is producer cell-dependent. J.Gen.Virol. 79 (Pt 10) (1998) 2447-2453.

[93] S.T. Valente, C. Chanel, J. Dumonceaux, R. Olivier, S. Marullo, P. Briand, U. Hazan, CXCR4 is down-regulated in cells infected with the CD4-independent X4 human immunodeficiency virus type 1 isolate m7NDK. J Virol 75 (2001) 439-447.

[94] S. Venzke, N. Michel, I. Allespach, O.T. Fackler, O.T. Keppler, Expression of Nef downregulates CXCR4, the major coreceptor of human immunodeficiency virus, from the surfaces of target cells and thereby enhances resistance to superinfection. J.Virol. 80 (2006) 11141-11152.

[95] J. Wang, G.J. Babcock, H. Choe, M. Farzan, J. Sodroski, D. Gabuzda, N-linked glycosylation in the CXCR4 N-terminus inhibits binding to HIV-1 envelope glycoproteins. Virology 324 (2004) 140-150.

[96] J. Wang, Y. Shiozawa, J. Wang, Y. Wang, Y. Jung, K.J. Pienta, R. Mehra, R. Loberg, R.S. Taichman, The role of CXCR7/RDC1 as a chemokine receptor for CXCL12/SDF-1 in prostate cancer. J.Biol.Chem. 283 (2008) 4283-4294.

[97] J.F. Wang, I.W. Park, J.E. Groopman, Stromal cell-derived factor-1alpha stimulates tyrosine phosphorylation of multiple focal adhesion proteins and induces migration of hematopoietic progenitor cells: roles of phosphoinositide-3 kinase and protein kinase C. Blood 95 (2000) 2505-2513.

[98] J.A. Werner, I.O. Rathcke, R. Mandic, The role of matrix metalloproteinases in squamous cell carcinomas of the head and neck. Clin.Exp.Metastasis 19 (2002) 275-282.

[99] A.T. Wierenga, I. Vogelzang, B.J. Eggen, E. Vellenga, Erythropoietin-induced serine 727 phosphorylation of STAT3 in erythroid cells is mediated by a MEK-, ERK-, and MSK1-dependent pathway. Exp.Hematol. 31 (2003) 398-405.

[100] S. Wildum, M. Schindler, J. Munch, F. Kirchhoff, Contribution of Vpu, Env, and Nef to CD4 down-modulation and resistance of human immunodeficiency virus type 1-infected T cells to superinfection. J.Virol. 80 (2006) 8047-8059.

[101] D. Wolf, V. Witte, B. Laffert, K. Blume, E. Stromer, S. Trapp, P. d'Aloja, A. Schurmann, A.S. Baur, HIV-1 Nef associated PAK and PI3-kinases stimulate Akt-independent Bad-phosphorylation to induce anti-apoptotic signals. Nat.Med. 7 (2001) 1217-1224.

[102] H. Yasuoka, M. Tsujimoto, K. Yoshidome, M. Nakahara, R. Kodama, T. Sanke, Y. Nakamura, Cytoplasmic CXCR4 expression in breast cancer: induction by nitric oxide and correlation with lymph node metastasis and poor prognosis. BMC.Cancer 8 (2008) 340.

[103] N. Yoshitake, H. Fukui, H. Yamagishi, A. Sekikawa, S. Fujii, S. Tomita, K. Ichikawa, J. Imura, H. Hiraishi, T. Fujimori, Expression of SDF-1 alpha and nuclear CXCR4 predicts lymph node metastasis in colorectal cancer. Br.J.Cancer 98 (2008) 1682-1689.

[104] J. Zak, S.W. Schneider, I. Eue, T. Ludwig, H. Oberleithner, High-resistance MDCK-C7 monolayers used for measuring invasive potency of tumour cells. Pflugers Arch. 440 (2000) 179-183.

[105] M. Zhao, D. Sano, C.R. Pickering, S.A. Jasser, Y.C. Henderson, G.L. Clayman, E.M. Sturgis, T.J. Ow, R. Lotan, T.E. Carey, P.G. Sacks, J.R. Grandis, D. Sidransky, N.E. Heldin, J.N. Myers, Assembly And Initial Characterization Of A Panel Of 85 Genomically Validated Cell Lines From Diverse Head And Neck Tumor Sites. Clin.Cancer Res.2011).

[106] A. Zlotnik, Chemokines in neoplastic progression. Semin.Cancer Biol. 14 (2004) 181-185.

8. Appendix

8.1 Abbreviations

AIDS	Acquired immunodeficiency syndrome
APCs	Antigen presenting cells
APS	Ammoniumpersulphate
BSA	Bovine serum albumin
CI	Cell index
CXCR4	C-X-C chemokine receptor type 4
DAPI	4',6'-diamidino-2-phenylindole, dihydrochloride
DMEM	Dulbecco’s Modified Eagle Medium
DMSO	Dimethylsulfoxide
DNase	Deoxyribonuclease
ECL	Enhanced chemiluminescence
ECM	Extracellular Matrix
EDTA	Ethylene diaminetetraacetic acid
ERK	Extracellular signal regulated kinases
FCS	Fetal calf serum
FITC	Fluorescein isothiocyanate
JAKs	Janus Kinase
HRP	Horseradish peroxidase
HIV-1(HIV-2)	Human immunodeficiency viruses 1 (or 2)
kDa	Kilodalton
MDCK-C7	Madine-Darby canine kidney cell-clone 7
mTOR	mammalian target of rapamycin
MW	Molecular weight
NP40	Nonidet P 40 substitute
PAGE	Polyacrylamide gel electrophoresis
PBS	Phosphate buffered saline

PCR	Polymerase Chain Reaction
rpm	Revolutions per minute
SDF-1α	Stromal cell-derived factor-1α
SDS	Sodium-Dodecyl-Sulphate
SIV	Simian immunodeficiency virus
STAT 3	Signal transducer and activator of transcription 3
STR	Short tandem repeat analysis
TEER	Transepithelial electrical resistance
TEMED	N, N, N', N'-tetramethyl ethylenediamine
WT	Wild type

8.2 Table index

8.3 Figure index

8.4 Presentations

- “**Differential expression of VEGF-A isoforms in angiomas and squamous cell carcinoma cell lines of the head and neck area.”**

  2nd International Symposium on Hemangiomas and Vascular Malformations of the Head and Neck, Little Rock, USA, 2009.

- **“SIV Nef as a new therapeutic approach in head and neck cancer.”**

  Workshop zur klinischen und experimentellen Forschung in der Kopf-Hals-Onkologie, Leipzig, Germany, 2011.

- **“Implications of SIV-Nef in antiangiogenesis.”**

  3rd International Symposium on Hemangiomas and Vascular Malformations of the Head and Neck, Marburg, Germany, 2011.

8.5 Curriculum vitae and publications

Name : *Chengzhong Cai*

Gender : *male*

Date of birth : *8th October 1974*

Marital status: *Married*

Tel : *(+49)-017634147136*

E-mail: *chengzhong.cai@gmail.com*

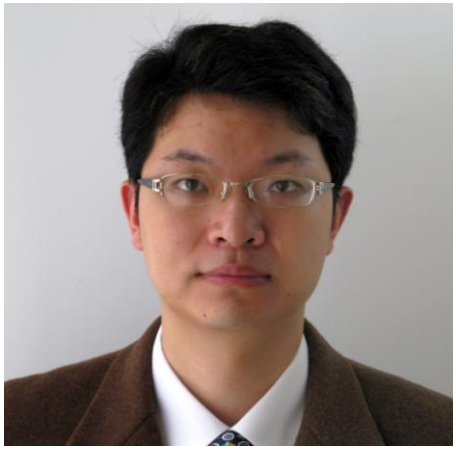

Education experience

- ***Medical College of Philipps-University, Marburg, Germany***

  October 2008 – present

  Doctoral thesis

- ***Medical College of TongJi University, Shanghai, China.***

  October 2004 – December 2006

  Master degree of Medicine –Surgery

- ***Changzheng Hospital, Shanghai, China.***

  September 2004 – April 2005

  Visiting scholar, Central Lab of Molecular Biology. Field of research: "The expression of E-cadherin in gastric cancer."

- ***Medical College of Tiedao University, Shanghai, China.***

  September 1993 – July 1998

  Bachelor degree of Medicine

Working experience

- ***University Hospital Giessen and Marburg, Marburg, Germany.***

  November 2008 – present

  Doctoral fellow of Prof. Mandic

- ***Shanghai Tenth People's Hospital, China.***

  2003 - November 2008

  Attending Doctor.

- ***Shanghai Tenth People's Hospital, China.***

  August 1998 – 2003

  Resident Doctor.

Qualifications

- ***Doctor's Qualification Certification of The People's Republic of China.***

  December 1999

- ***Doctor's Practice Certification of The People's Republic of China.***

  December 2001

- ***Qualification Certificate of Speciality and Technology of The People's Republic of China. (General Surgery)***

  September 2003

- ***Teacher's Qualification Certification (College level) in Clinical Medicine of The People's Republic of China.***

  January 2004

Membership

- *Chinese Medical Association*
- *Angioma group, University Hospital Giessen and Marburg, Germany*
- *German Society of Oto-Rhino-Laryngology, Head and Neck Surgery*

Publications

1. ***Cai C**, Böttcher MC, Werner JA, Mandic R. Differential expression of VEGF121, VEGF165 and VEGF189 in angiomas and squamous cell carcinoma cell lines of the head and neck. Anticancer Res. 2010; 30(3):805-10.*

2. *Martina C. Boettcher, Behfar Eivazi, Marion Roessler, Michael Bette, **Cai C**, Susanne Wiegand, Christian Güldner, Jochen A. Werner, Robert Mandic. Involvement of LYVE-1-positive endothelial cells in the formation of non-lymphatic vascular malformations. Histopathology. 2010; 57(5): 763–770.*

3. *Teng HF, Wang S, Ge HY, Zhu WH, **Cai C,** Jiang X. Thyroidectomy through suprasternal approach under endoscope. Joural of TongJi university(medical science). 2008; 6.*

4. *Ge HY, Hao ZH, Jiang SL, **Cai C**, Jiang X. The clinical experience of lobectomy of thyroid with small cervical incision. Journal of Endocrine Surgery. 2008; 2(1).*

5. ***Cai C**, Xu HW, Tan LY. To establish a method of semi-quantitative RT-PCR with two-step-circle in separated tube to detect E-cadherin levels in gastric cancer cells. China Clinic Cancer. 2006; 33(8): 4-6.*

6. ***Cai C***, *Xu HW, Tong XC. High Expression of E-cadherin in serum and tissues of colorectal Cancer. World Chinese Journal of Digestology. 2004; 12(6): 1481-1483.*

7. *Xu HW, Wang L, Tong XC,* ***Cai C.*** *Correlation between transforming growth factor ß1 and its receptor and stomach carcinoma aggressiveness. Acad J Sec Mil Med Univ. 2004; 25(10): 1149-1150.*

8. *Xu HW,* ***Cai C****, Tan LY. Relationshinp of serum and tissue E-cadherin levels and radical operation on stomach carcinomas. Chin J EXP Surg. 2003; 20(8): 751-752.*

9. *Xu HW,* ***Cai C****, Tong XC. The influence of aggressiveness and surgical operation of colorectal carcinomas on serum E-cadherin level. Cancer Research on Prevention and Treatment. 2003; 30(3): 190-191.*

10. *Xu HW,* ***Cai C****, Tan LY. The influence of aggressiveness on serum E-cadherin Level in patients suffering from stomach carcinoma. China Clinic Cancer. 2003; 30(8): 533-535.*

Language Skills:

- *English*
- *German*
- *Chinese*

8.6 List of academic teachers:

Main academic teachers in Tongji University, Shanghai, China.

Ms. / Mr :

Cai, Chen, Fan, Ge, Gu, Guo, Li, Liu, Luo, Wei, Xiong, Zhang

Main academic teachers in Philipps-University, Marburg, Germany.

Ms. / Mr :

Bette, Eivazi, Mandic, Ocker, Sesterhenn, Teymoortash, Weiß, Werner

8.7 Acknowledgements

I thank Prof. Dr. med. Jochen A. Werner for his kind financial support during these three years. Here, I want to show my great appreciation to my supervisor, Prof. Dr. med. Robert Mandic, for his patient education, kindly help and also for his strong pressure to keep me forward. I also thank my colleagues Ms. Roswitha Peldszus, Ms. Maria Sadowski, Ms. Annette Rossmann, Ms. Marie Meinold, Ms. Thuridur Jonsdottir, Ms. Galina Makarova, Ms. Branka Malidzan, Ms. Ariane Rath, Ms. Fiona Rodepeter, Mr. Christian Wiemers (Dept. of Otolaryngology, Head & Neck Surgery, UKGM GmbH) and our co-operators Priv. Doz. Dr. Michael Bette (Department of Anatomy and Cell Biology, Philipps-University Marburg, Germany), Mr. Thorsten Volkmann (Dept. of Hematology, Oncology and Immunology, UKGM GmbH), Prof. Dr. med. Matthias Ocker, Dr. med. Karl Quint and Dr. Pietro Di Fazio (Institute for Surgical Research, UKGM GmbH) for their excellent technical assistance. I also want to show my thanks to Prof. Dr. med. Afshin Teymoortash, Prof. Dr. med. Andreas Sesterhenn, Dr. med. Rainer Weiß, Dr. med. Behfar Eivazi and other doctors (Dept. of Otolaryngology, Head & Neck Surgery, UKGM GmbH) for their supports and kindly help during my practice in clinic.

At last but not least, I want to thank my family, especially my wife Hui Chen, I could not have succeeded without their support. I am dedicating my doctoral thesis as a gift to my new born daughter Ouchun Cai. I love you and miss you so much. I hope you will come back to Marburg when you grow up.

8.8 Ehrenwörtliche Erklärung

This part was removed since it contains personal data.